IISEE Lecture Note
2007-2008

# Earthquake Resistant Limit State Design

By

H. Akiyama


April 14 & 15, 2008

International Institute of
Seismology and Earthquake Engineering,
Building Research Institute

# Method Based on Energy Criteria

Hiroshi AKIYAMA
Real Estate Science
Graduate School of Science and Technology
Nihon University
Kanda-Surugadai, Chiyoda-ku, Tokyo, Japan

## 1. INTRODUCTION

### 1.1 Short History of Earthquake Resistant Design Method

Earthquake resistant design method in a sense of modern technology started immediately after the Great Kanto Earthquake (1923)(See Table 1.1). Since then, during three fourths century earthquake resistant design has made a great progress. As the scope of the applied structures was extended, the design ideas became versatile. As the electronic digital computers and apparatuses for field observation became available, analytical techniques for response analysis developed drastically and became versatile. On the other hand, successive attacks of big hazardous earthquakes made us continuously recognize the arrived level earthquake resistant design method to be still incomplete. The earthquake resistant design started as a measure by which a structure basically designed for gravity loading is to be supplied additionally with a resistance against earthquakes. Increased experiences of earthquake hazard and the progress of response analysis techniques have raized the importance of earthquake resistant design to such a extent that the design of structures is governed mostly by earthquake resistant design.

Under such a circumstance, a methodology to be perfectly free from dreadful hazard made by earthquakes has been sought after in realizing so-called "base-isolated structures." Such a methodology, however, had to wait the chance of germination for about a half century in the shade of a steady development of earthquake resistant design method. In order to establish a base-isolated structure, matured design theory and reliable structural element such as the laminated rubber bearing which appeared in 1970's had to be prepared as preconditions.

The development of earthquake resistant design and realization of base-isolated structured, however, did not developed favorably without any obstacles and each had to go through hardships. One of the reason is that the earthquake resistant design in Japan assumed from the start a character of law to be observed for the public welfare. On one hand, the earthquake resistant design must be rational one supported by scientific grounds and, on the other hand, it must be equipped with a lucid logic. The scientific fact and a logic, however, are not same. Incorrect recognition of a fact can be always stated logically. This basic contradiction lying under the earthquake resistant design has been the cause of a tenaciously made long dispute. This dispute is called the dispute about "flexible or stiff", which started immediately after the introduction of the lateral force method and raised a question on the recommended principle, at that time, that structure should be stiff. Although the lateral force method is superior in its practicability and logical consistency, it is not perfect scientifically.

The lateral force method has been established during the period of introducing nuclear power

Table 1.1 Historical Background

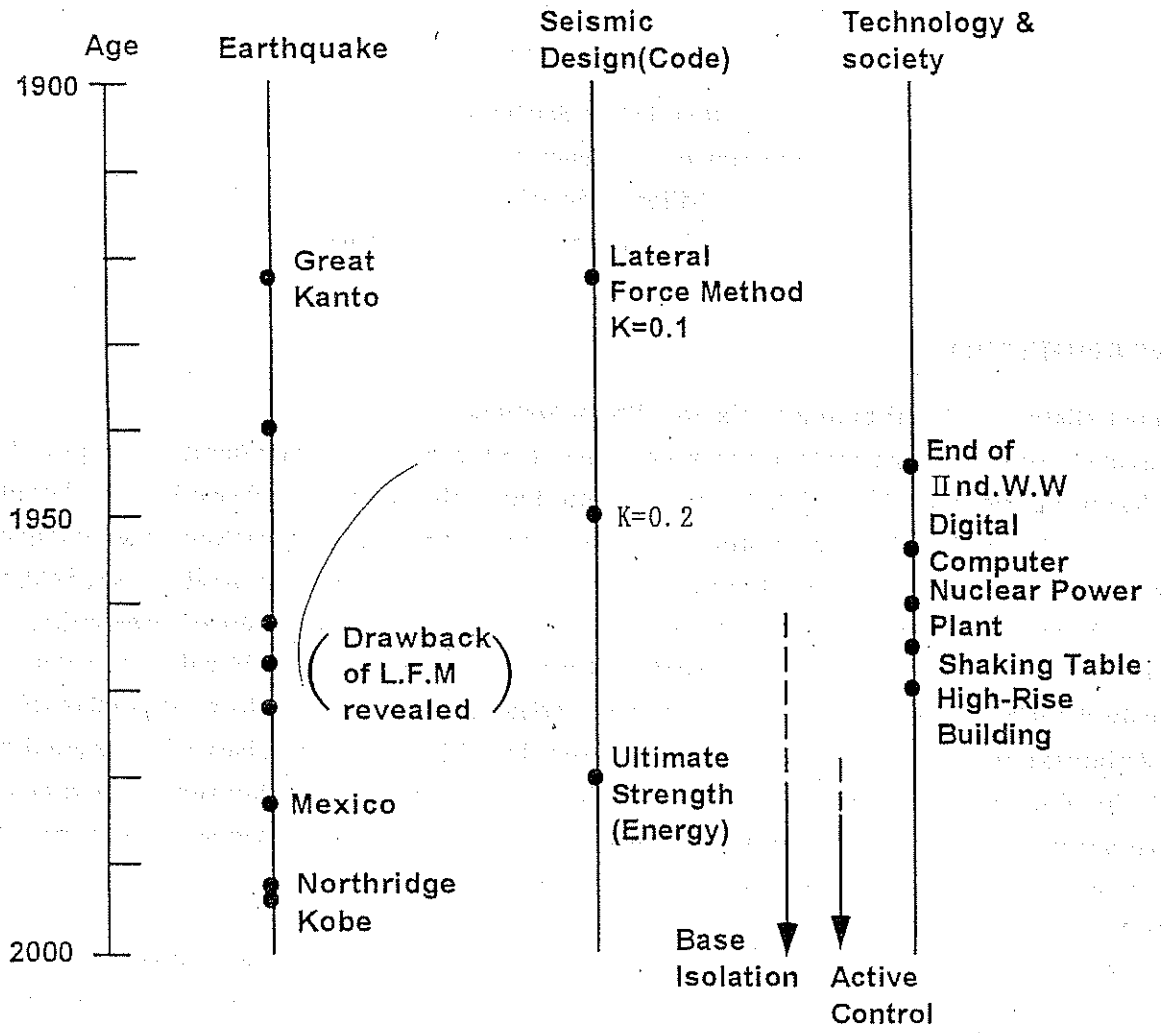


plants and drastic economic growth in Japan as a design methodology that the important structures should be designed stiff and strong. A high rate of economic growth in late 1960's promoted raising the height of buildings in urban areas, and the possibility of super high-rise buildings in highly seismic countries were discussed in the second dispute about "flexible or stiff". As a result, it was made clear that as the natural period of a structure increases, seismic force applied to the structure reduces reversely proportional to the natural period. Thus, the side of "flexible" triumphed.

As the development of computers and techniques of field observation brought about more detailed knowledge of structural behavior under earthquakes, also, it has been made clear that the structures with intermediate height can receive far stronger seismic forces than that prescribed by the lateral force method. Comings of the Niigata Earthquake (1963), the Tokachi-oki Earthquake (1968) and the Miyagiken-oki Earthquake (1973) made us realize the insufficiency of the lateral force method. Then, the third theme of the dispute was how to endow a structure with a sufficient energy absorption capacity.

In 1981, the Japanese building code was revised to cope with the energy absorption capacity.

In addition to the previous lateral force method, the energy absorption capacity was introduced as a basic performare which should be equipped with a structure to resist to earthquakes.
By this, the basic framework of seismic design in which the basis requirement of force by the lateral force method was supplemented with the requirement of deformation capacity, was established.
How to secure the deformation capacity, however, is a matter concerned with the nonlinear field beyond the elastic limit and can not be easily implemented even by applying advanced modern technologies. Even more as the analytical tools are well prepared, we should be confronted with the situation in which we are bewildered by getting too many options and losing objective measures to judge the validity of the results of analysis.
The main theme of the third dispute about "flexible or stiff" can be said to be a pragmatic problem about how to reflect the energy absorption capacity in the inelastic range to the seismic design in general. At the same time, also, in this period, as an opponent to the earthquake resistant design which dashed forward to the way of complication, the base-isolated structure, which aims to escape fundamentally from the devastative damage, began to be seriously discussed of its real applicability in Japan.
The earthquake resistant structures are expected to develop both the strength and deformation capacity as required to resist earthquake. Therefore, it is inevitable that structural skeletons suffer some damage under an attack of an earthquake. Contrary to this, the base-isolated structure challenged the earthquake resistant structure, asserting that the structural skeletons should be made free of any damage. For this assertion, the circle of the earthquake resistant design hardly understood the true meaning, still keeping the standpoint that the possibility of base-isolated structures couldn't be proven in such a highly seismic country as Japan. On the other hand, in spite of tenacious resistance of the circle of the earthquake resistant design, the circle of the base-isolated structures at last succeeded to prove the applicability, based on the same ground as that on which the earthquake resistant design stands.
To be able to do so, the appearance of the excellent structural element such as "laminated rubber isolater" was inevitably necessary.
The principle of the base-isolated structure can be recognized as follows.

> The base-isolated structure is a dual structure, in which the building part forms a superstructure and the base-isolating layer and foundations form a substructure. The base-isolating layer is formed with a group of laminated rubber isolaters which acts as a flexible elastic part and with a group of dampers which acts as a stiff energy absorbing part. Since the rigidity of the superstructive is sufficiently stiff compared to that of the substructure, the base-isolated structure is identified to be a one-mass system.

The high vertical-load bearing capacity and the large elastic deformation capacity of the laminated rubber bearings enable the base-isolated structure to be equipped with a natural period longer than 4.0sec, and the base-isolating layer can behave as a highly efficient energy absorbing mechanism due to a favorable combination of elasticity of isolators and plasticity of dampers.
The base-isolated structure is equipped with simplicity and clarity which should be intrinsic in the true earthquake resistant structure.
Moreover, it is equipped with advantageous characteristics of the long-period structure, and the uncertainty in damage distributions is basically removed in the base-isolated structure in which the seismic energy input is totally absorbed in the base-isolating layer. Although the base-isolated

structure just emerged as an opposing concept to the earthquake resistant structure, through the fourth dispute on "flexible or stiff", it was proven to be an excellent earthquake resistant structure. On the other hand, ordinary earthquake resistant structures, structural skeletons of which are designed primarily to support gravity loading and are utilized also to develop the strength and energy absorption capacity required to resist to earthquakes, have a fundamental deficiency to be simple and clear structures.

Just then, at dawn of January, 17th in 1995, The Hyogoken-Nambu Earthquake happened and taught us the real level of earthquake resistant structures at present.

The intensities of ground motions in the epicentral zone were partly far greater than that prescribed by Japanese building code. Observed various sorts of damage, however, made us feel that the goal of seismic design is still far away. Two base-isolated buildings constructed not so far from the epicentral zone were proven to have developed an anticipated performance.

The seismic design of 20th century is closing in rise and flourish of base-isolated structures. It is, however inconceivable that all buildings would turn to be base-isolated structures. The earthquake resistant structures will make a strenuous effort toward a breakthrough, awakened by superiority of base-isolated structures.

And also, the base-isolated structures would change qualitatively with an enormous increase of their application. In any way, the fifth dispute about "flexible or stiff" would develop on the axis of base-isolated structure.

This dispute must be a hard and desperate battle for the earthquake resistant structure.

### 1.2 Importance of Energy Concept [1)]

In order to know the process of collapse of structures subjected to earthquakes, a high nonlinearity of structures must be analysed by using the equation of motion. Although the obtained results are specific and isolated solutions, characterized strongly by specific conditions, these results can be synthesized through the equation of energy balance which is obtained by multiplying a displacement increment on both sides of the equation of motion and by integrating over the duration of the ground motion.

The reason is;

- Information is integrated through integration.
- The energy is a scaler composed by the product of force and deformation and is a suitable quantity for synthesis.
- The seismic energy input in total is a stable amount which depends mainly on the total mass and the fundamental natural period of a structure as predicted by Housner [2)].

As far as the total energy input is a stable constant quantity, the major concern in the seismic design should be focussed on the manner in which the input energy is distributed over a structure.

The equation of motion for one-mass system is written as

$$M\ddot{y}+C\dot{y}+F(y) = -M\ddot{z}_0 \tag{1.1}$$

where $M$ : mass

$y$ : relative displacement of the mass

$C$ : damping coefficient

$F(y)$ : restoring force

$\ddot{z}_0$ : ground acceleration

Eq(1.1) expresses a fundamental relationship which governs the vibrational response and any responses can be obtained by integrating the equation.

By multiplying $dy$ to Eq(1.1) and integrating over the duration of ground motion, the equation of energy balance is obtained as follows.

$$\int_0^{t_0} M\ddot{y}\dot{y}dt + \int_0^{t_0} C\dot{y}^2dt + \int_{y(0)}^{y(t_0)} F(y)dy = -\int_0^{t_0} M\ddot{z}_0\dot{y}dt \tag{1.2}$$

Eq(1.2) can be written also as

$$W_e + W_p + W_h = E \tag{1.3}$$

where $W_e$ : elastic vibrational energy

$W_p$ : cumulative inelastic strain energy

$W_h$ : energy absorbed by damping

$E$ : total energy input exerted by an earthquake

Eqs.(1.1) and (1.2) are easily extended to apply to multi-mass systems by expressing related quantities with matrices and vectors.

Eq.(1.1) expresses a balance of force at an instant and the numerical integration of Eq.(1.1) yields structural responses at any level of structural damage irrespective of structural states to be elastic or elastic.

The obtained information is scattered and discrete one governed by specific conditions.

Only one guarantee for exactness of results obtained by Eq.(1.1) is given by a proper execution of numerical calculation, and Eq.(1.1) does not speak much of the structural behavior under earthquakes.

On the other hand, Eq.(1.2) or Eq.(1.3), which is also an exact expression of structural responses, can speak generally about various phases of structural behavior in terms of $W_e$, $W_p$ and $W_h$.

Moreover, the stable nature of the total energy input stated below enhances the applicability of Eqs.(1.2) and (1.3).

> The total energy input exerted by an earthquake is mainly governed by the total mass and the fundamental natural period of a structure and is hardly influenced by design parameters such as the strength distribution, mass distribution, and stiffness distribution.

As a basis of design consideration, deep understanding for the real behavior of structures under earthquakes is indispensable. In order to store knowledge, it is effective to accumulate individual results obtained by Eq.(1.1) by means of Eq.(1.3). Through this procedure, the relationship between the seismic input and the structural response can be synthetically grasped and the practical measure to realize the structural performance which is aimed by structural designers can be explicitly shown.

The design method based on Eq.(1.3) grounded by enormous amount of results of numerical analyses made by Eq.(1.1) can cope with the general design judgements. In this sense, this design method can be called a general design method or a synthetic design method.

The required structural performance of a structure is originally claimed by the owner of the structure. Therefore, the design method can be stated by a language which can be understood not only engineers but also laymen. Since the synthetic design method can be spoken by a plain language, the significance of synthesis in constructing a system of technical language can not be disregarded.

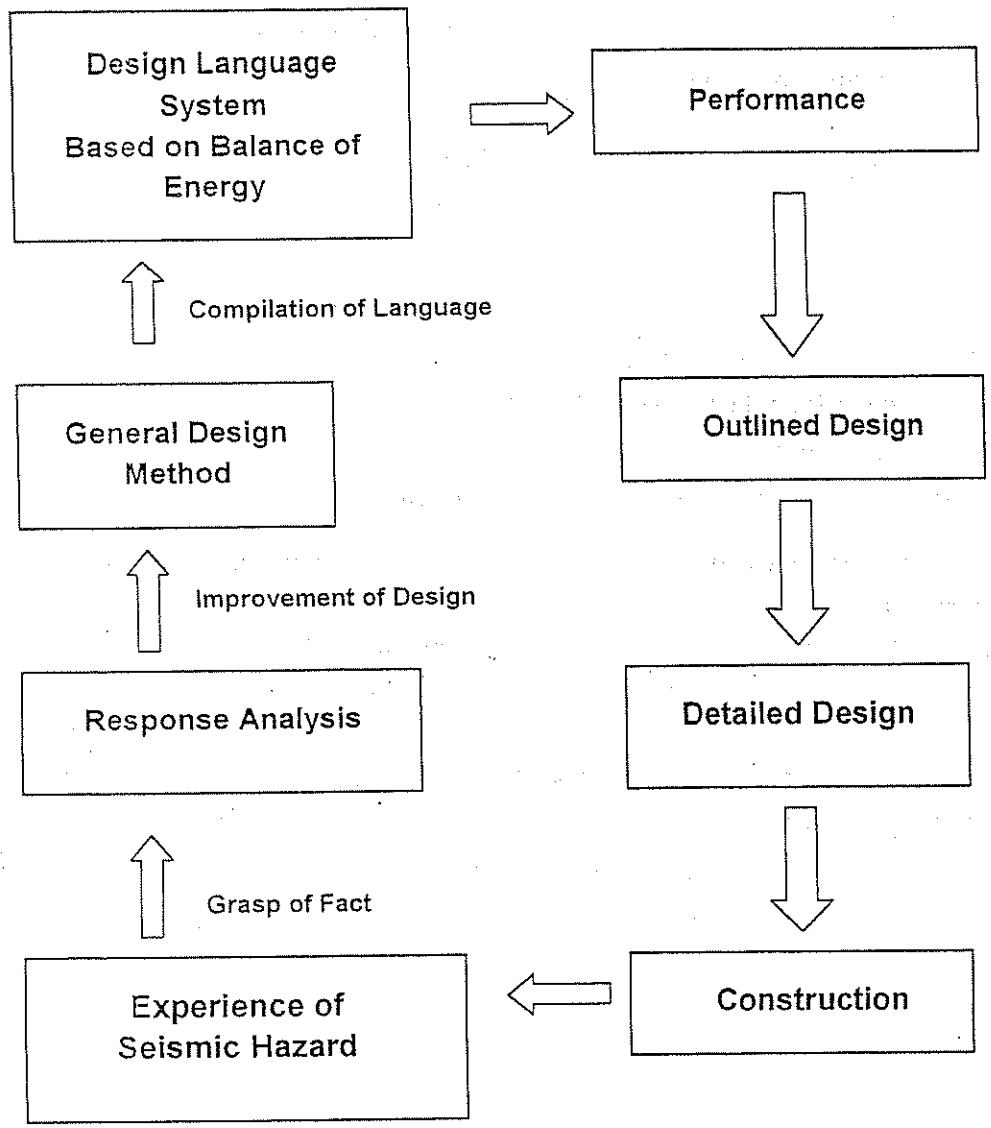


Fig.1.1 Development of Seismic Design

An outlined design can be made using the design language and the general design method as shown by Fig.1.1.

In the process of the detailed design, sometimes, the numerical response analysis is required to prove the fulfillness of structural performances.

The numerical response analysis is useful to improve the applicability of the general design method and, then, to improve the design language.

In such a manner, repetition of the analysis and synthesis and the accumulation of experiences of seismic hazard will lead to the progress of the earthquake resistant design method.

## 2 Energy Input in Single-Degree of Freedom System.

### 2.1 Equilibrium of Force and Equilibrium of Energy

The equation of equilibrium of the one-mass system shown in Fig.2.1(a) is expressed as

$$M\ddot{y}+C\dot{y}+F(y)=F_e \tag{2.1}$$

where $M$ : mass

$C\dot{y}$ : damping force

$F(y)$ : restoring force

$F_e$ : seismic force

$Z_0$ : horizontal motion of the ground

$y$ : displacement of the mass relative to the ground

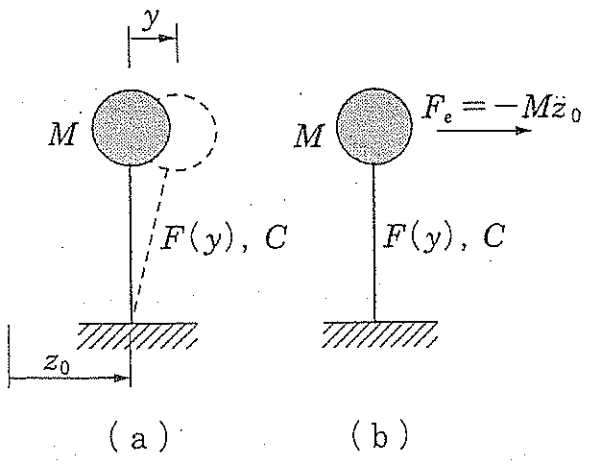


Fig.2.1 One-mass Vibrational System

Eq.(2.1) can be also applied to the system which stands on the fixed ground and is subjected to the force, $F_e$ applied on the mass. The response of the system can be obtained by integrating Eq.(2.1). Whereas the analytical closed form of solution is obtained for elastic systems, Eq.(2.1) is generally solved by means of numerical analysis for the plastified systems. When the solution is obtained, the equilibrium of force stated by Fig2.1(b) can be transformed to the equilibrium of energy. The important response is the relative displacement, $y$. $y$ causes strains in the system. Also, with respect to energy, the energy which is associated with strain is important in structural design point of view. Therefore, herewith, the equilibrium of energy is evaluated for the model shown by Fig.2.1(b), by multiplying $dy$ $(=\dot{y}dt)$ to Eq.(2.1).

The equilibrium equation is written as

$$M\int_0^t \ddot{y}\dot{y}dt+C\int_0^t \dot{y}^2dt+\int_0^t F(y)\dot{y}dt=\int_0^t F_e\dot{y}dt \tag{2.2}$$

The constituent of Eq.(2.1) is discriminated as follows.

$$E(t)=\int_0^t F_e\dot{y}dt \tag{2.3}$$

$$W_e(t)+W_p(t)=M\int_0^t \ddot{y}\dot{y}dt+\int_0^t F(y)\dot{y}dt \tag{2.4}$$

$$W_h=C\int_0^t \dot{y}^2dt \tag{2.5}$$

where $E(t)$ : energy input at the time of $t$

$W_e(t)$ : elastic vibration energy at the time of $t$

$W_p(t)$ : cumulative inelastic strain energy at the time of $t$

$W_h(t)$ : energy absorption due to damping at the time of $t$

The elastic vibration energy $W_e$ can be written as

$$W_e(t)=W_{es}(t)+W_{ek}(t) \tag{2.6}$$

where $W_{es}(t)$ : elastic strain energy

$W_{ek}(t)$ : kinetic energy

The first term of the left hand side of Eq.(2.4) expresses, $W_{ek}(t)$. Considering $\dot{y}(0)=0$, $W_{ek}(t)$ is written as

$$W_{ek}(t)=\frac{M\dot{y}^2(t)}{2} \tag{2.7}$$

Therefore, the second term of the right-hand side of Eq.(2.4) is expressed as

$$W_{es}(t)+W_p(t)=\int_0^t F(y)\dot{y}dt \tag{2.8}$$

$t_0$ being the duration of the ground motion, the quantities at the time of $t_0$ are defined as follows.

$$\left.\begin{aligned} E&=E(t_0)\\ W_e&=W_e(t_0)\\ W_p&=W_p(t_0)\\ W_h&=W_h(t_0)\end{aligned}\right\} \tag{2.9}$$

where $E$ : total energy input

$W_e$ : elastic vibrational energy

$W_p$ : cumulative inelastic strain energy

$W_h$ : energy absorption due to damping

Eq.(2.2) is rewritten as

$$W_e+W_p+W_h=E \tag{2.10}$$

Eq.(2.10) is the fundamental equation on which the earthquake design method is constructed. Similar to Eq.(2.1), Eqs.(2.2) and (2.10) are equations of exact equilibrium. Eq.(2.1) provides structural responses. On the other hand, Eqs.(2.2) and (2.10) do not provide structural responses directly, but are very helpful to express and interpret structural responses.

The reasons are; whereas Eq.(2.1) expresses a state of equilibrium of force at an instant, Eqs.(2.2) and (2.10) provide an integrated information of vibrational state. Moreover, the effectiveness of Eq.(2.10) is guaranteed by the stability of the total energy input.

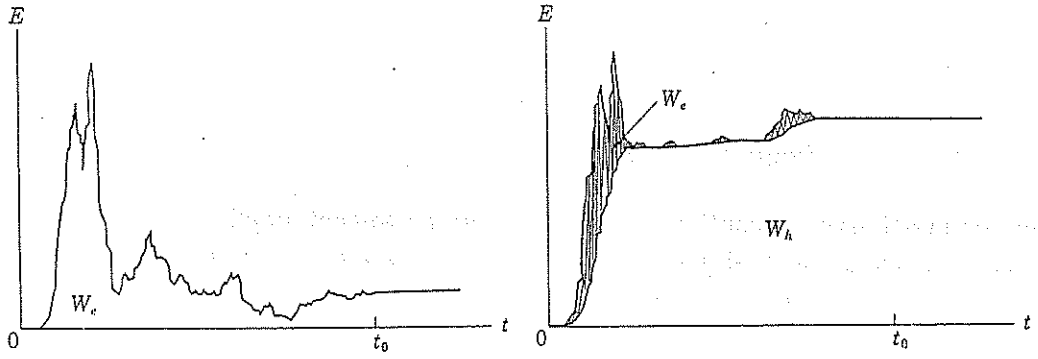


(a) purely elastic system (b) damped elastic system

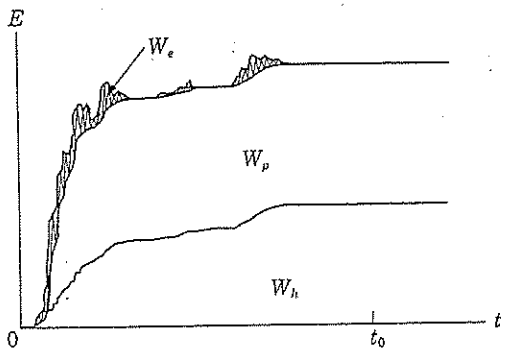


(c) inelastic system

Fig.2.2 Time History of Energy

Fig2.2 indicates the structural responses in time histories of energy. Fig2.2(a) indicates the case of an undamped system, in which the response is all elastic vibrational energy.

The energy input, $E(t)$ being always positive, is not necessarily increasing as time passes. Under $t$ greater than $t_0$, $E(t)$ is kept to be $E$, since the ground motion which adds energy input does not exist any more. The purely elastic system continues to vibrate under a constant energy input, $E$.

Fig 2.2(b) is a case of damped elastic system. The energy absorption due to damping, $W_h(t)$ is monotonously increasing. Therefore, as the damping factor increases, $E(t)$ tends to be monotonously increasing. The displacement response, $y$, reaching the maximum at a time within $t_0$, rapidly reduces to zero.

Fig.2.2(c) is a case of elastic-plastic system. The cumulative inelastic strain energy, $W_p(t)$ is also monotonously increasing. The absorbed energy due to damping becomes smaller than that absorbed by the elastic system with same damping coefficient, $C$.

## 2.2 Fundamental Characteristics of Energy Input

### 2.2.1 Energy Input in Undamped Elastic System

The vibrational equation of the undamped elastic system is given by the following equation.

$$M\ddot{y}+ky = -M\ddot{z}_0 \tag{2.11}$$

where $k$ : spring constant

Under the initial condition of $y(0) = \dot{y}(0) = 0$, Eq.(2.11) is solved by using Duhamel integral as follows.

$$\dot{y}(t) = -\int_0^t \ddot{z}_0(\tau)\cos\omega_0(t-\tau)d\tau \tag{2.12}$$

where $\omega_0$ = circular frequency $= \sqrt{k/M}$

The undamped elastic system continue to oscillate with a constant amplitude after the ground motion fades away as shown in Fig2.2(a). Then, the total energy input can be obtained by using the maximum velocity amplitude, $\dot{y}_{max}$ as follows.

$$E = \frac{M\dot{y}_{max}^2}{2} \tag{2.13}$$

The response at $t$ longer than $t_0$ is obtained from Eq.(2.12) as follows.

$$\dot{y} = \left(-\int_0^{t_0} \ddot{z}_0(\tau)\cos\omega_0\tau d\tau\right)\cos\omega_0 t + \left(-\int_0^{t_0} \ddot{z}_0(\tau)\sin\omega_0\tau d\tau\right)\sin\omega_0 t \tag{2.14}$$

Therefore $\dot{y}_{max}$ is given by

$$\dot{y}_{max} = \sqrt{a^2+b^2} \tag{2.15}$$

where $a = \int_0^{t_0} \ddot{z}_0(\tau)\cos\omega_0\tau d\tau$

$b = \int_0^{t_0} \ddot{z}_0(\tau)\sin\omega_0\tau d\tau$

$a$ and $b$ in Eq.(2.15) are called Fourier integral. The meaning of this integral is to extract the wave component characterized by the circular frequency, $\omega_0$ among wave components which composes the ground motion, $\ddot{z}_0$.

Therefore, Eq.(2.15) tells that the wave component which exerts energy input to an undamped elastic system is limited to a single wave component characterized by $\omega_0$.

Vibration of the undamped elastic system becomes resonant under a stationary sinusoidal input with $\omega_0$. This fact is common to the fact shown by Eq.(2.15) Thus, the undamped elastic system receives the energy very selectively.

The total energy input is transformed into an equivalent velocity by applying the following equation.

$$E = \frac{MV_E^2}{2}, \quad \left(V_E = \sqrt{\frac{2E}{M}}\right) \tag{2.16}$$

where $V_E$ : equivalent velocity of the total energy input

$V_E$ is the square root of the total energy input per unit mass, having an understandable dimension of velocity. The relationship between $V_E$ and $\omega_0$ (otherwise $f = \omega_0/2\pi$ or $T_0 = 2\pi/\omega_0$, $f$ : natural frequency, $T_0$ = natural period) is called energy spectrum. The energy spectrum of the undamped elastic system coincides with the so-called Fourier Spectrum.

### 2.2.2 Energy Input in Elastic Damped System

The second and third terms of the left-hand side of Eq.(2.1) are combined to express a quantity, $R$. The relationship between $R$ and $y$ is depicted schematically for the elastic undamped system, the damped elastic system and the inelastic system as shown in Fig.2.3. Fig.2.3(a) is for the case of purely elastic system. The $R-y$ relationship for the damped elastic system increases nonlinearity as $C$ increases.

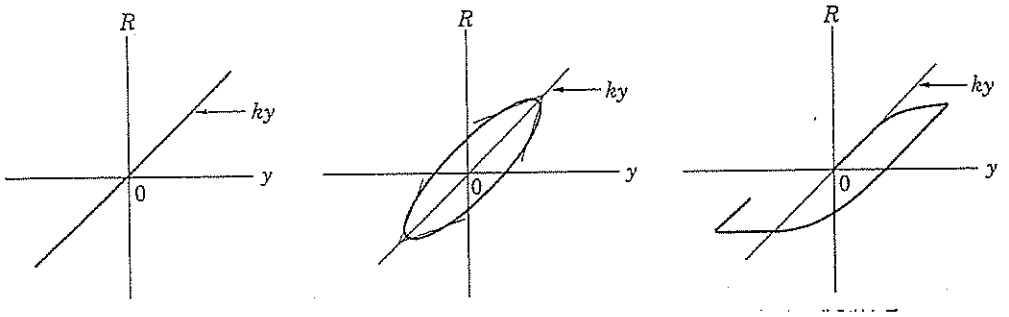


(a) purely elastic system (b) damped elastic system (c) inelastic system

Fig.2.3 $R-y$ Relationship

The free vibration of a damped elastic system is expressed by

$$\ddot{y}+2h\omega_0\dot{y}+\omega_0^2 y = 0 \tag{2.18}$$

where $h = C/2M\omega_0$ : damping constant

Under the initial condition of $y = y_0$ and $\dot{y} = 0$, the free vibration is obtained as

$$y = \frac{y_0}{\sqrt{1-h^2}} e^{-h\omega_0 t} \cos\left(\sqrt{1-h^2}\,\omega_0 t-\varepsilon\right), \quad \tan\varepsilon = \frac{h}{\sqrt{1-h^2}} \tag{2.19}$$

the period of free vibration is given by

$$T = \frac{2\pi}{\sqrt{1-h^2}}\sqrt{\frac{M}{k}} \tag{2.20}$$

The period given by Eq.(2.20) almost coincides with the natural period of the undamped elastic system, $T_0 = 2\pi\sqrt{M/k}$. The tangent slope in Fig.2.3(b), $k_t$, however, varies around $k$.
The instantaneous period, $T_t$ is defined to be

$$T_t = 2\pi\sqrt{\frac{M}{k_t}} \tag{2.21}$$

$T_t$ lies in the range of

$$T_0-\Delta T \leq T_t \leq T_0+\Delta T \tag{2.22}$$

$\Delta t$ which indicates the band of variation of $T_t$ increases as $h$ increases.
$h$ and $\Delta T$ are roughly related by the following relationship [1].

$$\Delta T = 1.5hT_0 \tag{2.23}$$

Therefore, the damped elastic system is characterized by a band of vibrational periods, while the purely elastic system is characterized by the single period of $T_0$. In this manner, as the vibrational system becomes complex, the wave components which supply energy to the system are plurallized. On the assumption that each wave component supplies energy evenly, the energy input in the damped elastic system can be calculated on the basis of the energy spectrum for the undamped elastic system, ${}_0V_E(T_0)$ as follows.

$$E = \frac{M\int_{T_0-\Delta T}^{T_0+\Delta T} {}_0V_E^2\, dT}{2\cdot 2\Delta T} \tag{2.24}$$

### 2.2.3 Energy Input in Inelastic System

The energy input for the system with $R = F(y)$ is discussed. The $R-y$ relationship is shown in Fig.2.3(c), where the initial slope is $k$ and the instantaneous vibration period is elongated as the inelastic deformation develops. Then, the band of variation of vibrational period is expressed as follows, taking the width of band to be $2\Delta T$, similarly to the case of damped elastic system.

$$T_0 \leq T \leq T_0+2\Delta T \tag{2.25}$$

where $T$ : substantial vibrational period

Therefore, the energy input in the inelastic system can be expressed as follows, similarly to the case of damped elastic system.

$$E = \frac{M\int_{T_0}^{T_0+2\Delta T} {}_0V_E^2(T)\, dT}{2\cdot 2\Delta T} \tag{2.26}$$

Thus, the energy input of the damped elastic system and that of the inelastic system are basically identical and can be calculated through averaging the energy input of the purely elastic system within a band width of period which corresponds to the variation of substantial vibrational period of each system.

### 2.2.4 Shape of Energy Spectrum

In this chapter, the major characteristics stated in 2.2.1 to 2.2.3 are ascertained and observed minutely.

Used ground motion records are;

- El centro record of the Imperial Vallay Earthquake (1940)
- Hachinohe record of the Tokachioki Earthquake (1968)
- Kobe Marine Observatory record of the Hyogoken-nanbu Earthquake (1995)

In Fig.2.4, the energy spectra for elastic systems are shown. It is clearly seen from the figure that as the damping is increased, the effect of averaging is deepened. The energy spectrum for the purely elastic system is highly dependent on the period. On the other hand, the energy spectrum

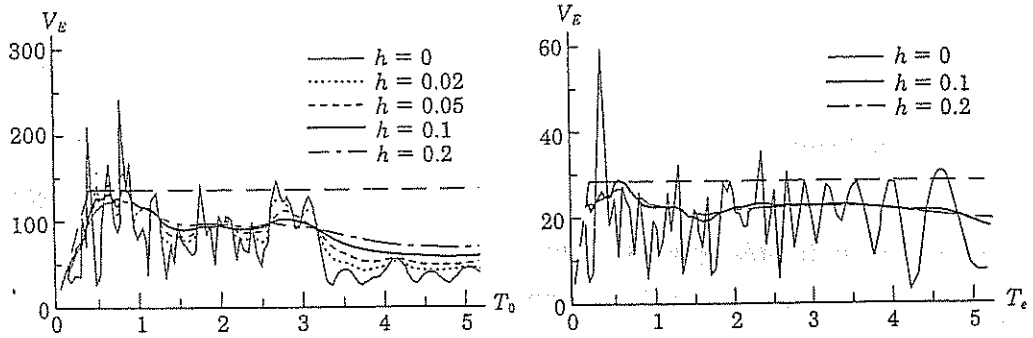


(a1) horizontal ground motion (a2) vertical ground motion

(a) El Centro record

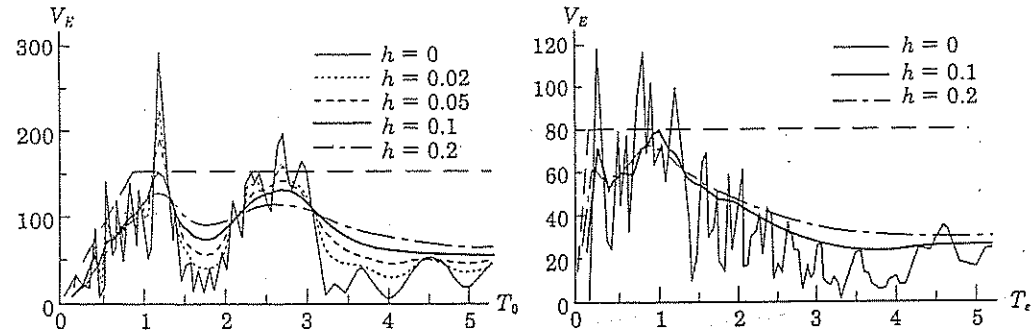


(b1) horizontal ground motion (b2) vertical ground motion

(b) Hachinohe record

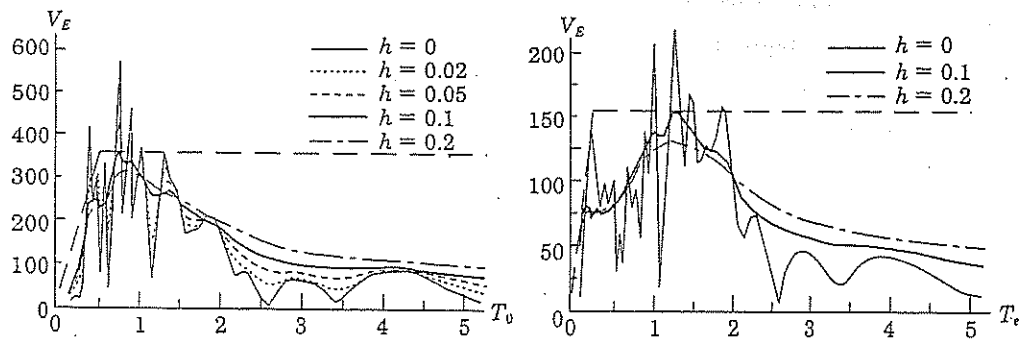


(c1) horizontal ground motion (c2) vertical ground motion

(c) Kobe Marine Observatory record

Fig.2.4 Energy Spectra for Elastic System

for the highly damped systems is not so dependent on the period. In each figure, the bi-linear type of spectrum which envelopes the energy spectrum for the damping of $h = 0.1$ is depicted by a broken line. As is stated in 2.2.6, the energy spectrum for the damping of $h = 0.1$ has an importance to be a design spectrum. The envelope of the energy-spectrum with $h = 0.1$ has a shape as shown in Fig. 2.5. According to the range of period, the simplified energy spectrum can be described as fol-

lows.

$T \leq T_G$ (shorter period range)

$$V_E = aT = \frac{V_{Em} T}{T_G} \tag{2.27}$$

$T > T_G$ (longer period range)

$$V_E = V_{Em} \tag{2.28}$$

where $T_G$ : period which divides ranges of period

$V_{Em}$ : maximum value of energy spectrum

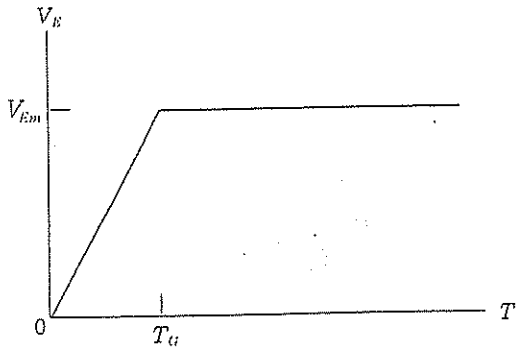


Fig.2.5 Shape of Energy Spectrum

In the range of longer period, $V_E$ fluctuates as $T$ increases, characterized by hills and valleys. The positions of hills and valleys, however, differ for different ground motions. As a result, a general shape in the range of longer period should be taken to be flat.

Next, the energy spectra for inelastic systems are discussed.

Used restoring force characteristics are shown in Fig.2.6 and these are;

- elastic-perfectly plastic type
- origin-orienting type
  (applicable to the reinforced concrete shear walls)
- degrading type
  (applicable to steel cylindrical shells)

The extent of plastification is expressed by the plastic deformation ratio defined. The apparent plastic deformations are defined as follows.

$$\delta_{pm}^{\pm} = \delta_m^{\pm} - \delta_Y \tag{2.29}$$

where $\delta_{pm}^{\pm}$ : apparent plastic deformations in positive and negative directions

$\delta_m^{\pm}$ : maximum deformations is positive and negative directions

The plastic deformation ratio is defined as follows.

$$\mu^{\pm} = \frac{\delta_{pm}^{\pm}}{\delta_Y} \tag{2.30}$$

$$\bar{\mu} = \frac{\mu^{+} + \mu^{-}}{2} \tag{2.31}$$

where $\bar{\mu}$ : average plastic deformation ratio

$\mu^{\pm}$ : plastic deformation ratios in positive and negative directions

In inelastic system, by adjusting the level of $Q_Y$, the aimed response of $\bar{\mu}$ can be easily obtained. First, $\bar{\mu}$ is fixed to be a certain value. Next, the response of $\bar{\mu}$ is calculated by Eq.(2.1). When the obtained response of $\bar{\mu}$ is smaller than the aimed value, the revised response of $\bar{\mu}$ closer to the aimed value is obtained by reducing $Q_Y$ by a suitable amount. Thus, after several times of trials, the aimed value is obtained, since the total energy input is a very stable amount.

In Fig.2.7, the total energy energy input in the inelastic system obtained for a specified value of $\bar{\mu}$ is indicated. In Figs.2.7(a1), (b1) and (c1), $V_E$ is depicted for $T_0$. A general tendency that the extent of averaging is deepened with the increase of $\bar{\mu}$ is clearly seen in reduction of undulation of energy inputs with the increase of $\bar{\mu}$.

In the range of shorter period, the averaging of energy spectrum, ${}_0V_E$ is made on the left hand side of $T_0$ as shown in Eq.(2.26). Thus, when the averaged value of $V_E$ is depicted on the abscissa of $T_0$, it is anticipated that $V_E$ increases with the increase of $\bar{\mu}$. Such a tendency is also clearly seen in Fig.2.7. In case of the elastic-perfectly plastic type of restoring force characteristics, this tendency is not remarkable. In other two cases, however, the increasing tendency of $V_E$ is so remarkable that the energy spectrum for the elastic system with the damping of $h = 0.1$ can not be a spectrum enveloping the energy input for inelastic systems in the range of shorter period.

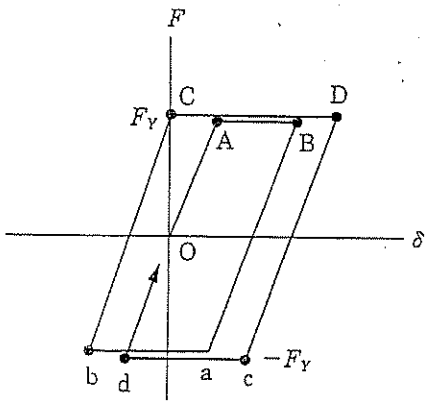


(a) elastic-perfectly plastic type

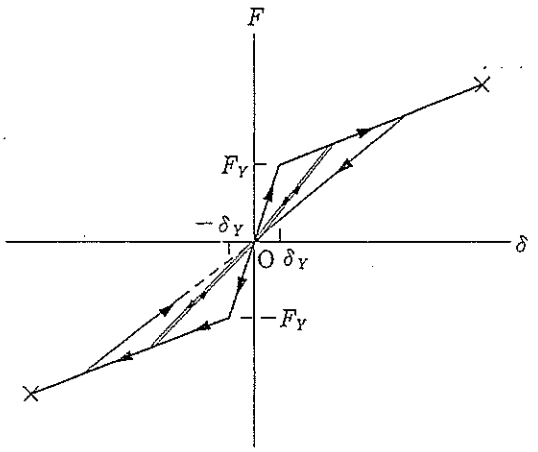


(b) origin-orienting type

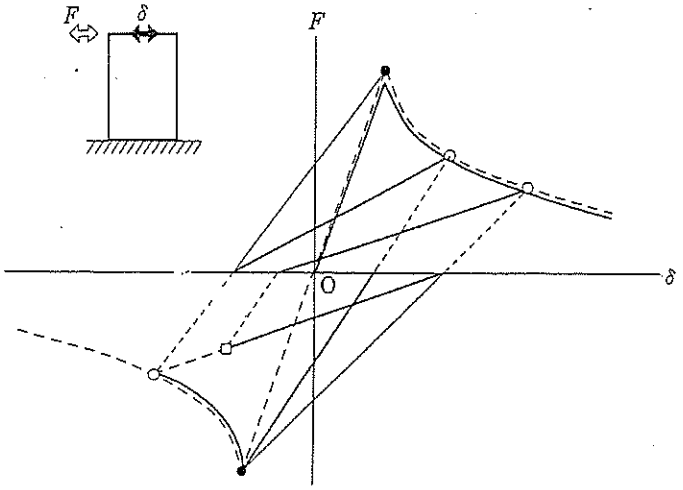


(c) degrading type

Fig.2.6 Types of Restoring Force Characteristics

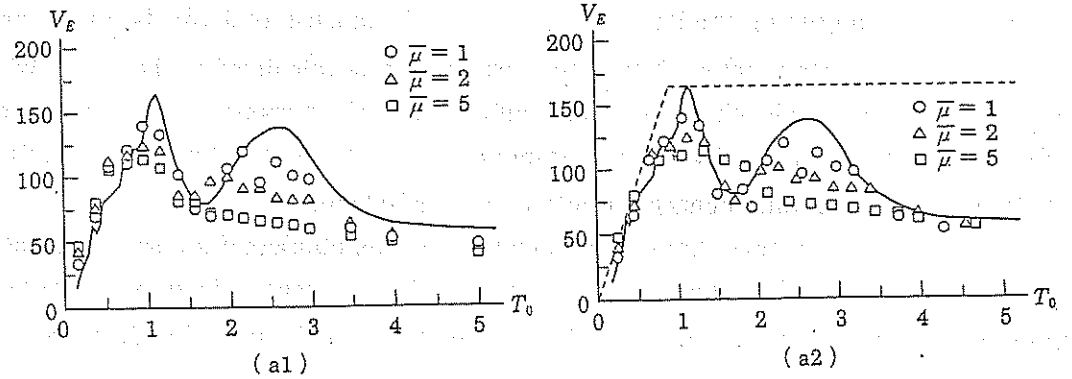


(a) elastic-perfectly plastic type

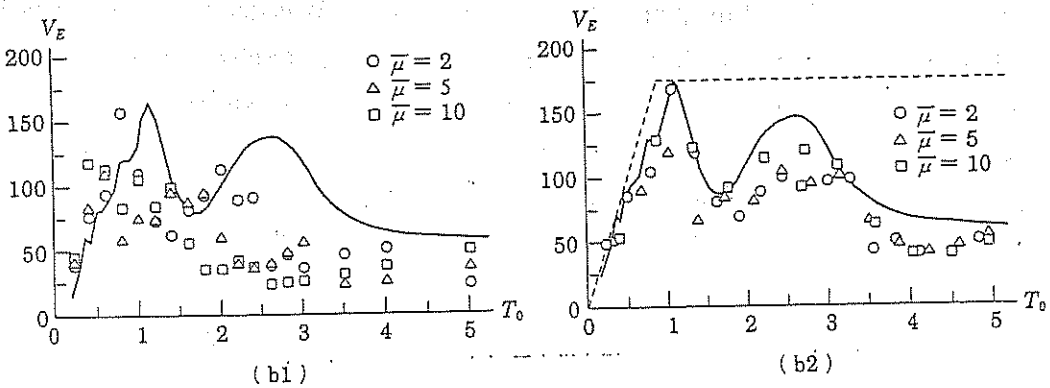


(b) origin-orienting type

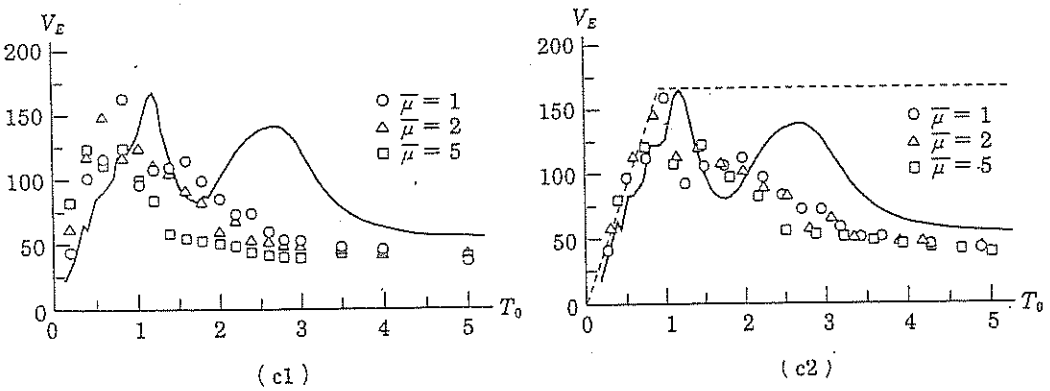


(c) degrading type

Fig.2.7 Energy Input in Inelastic System

### 2.2.5 Concept of Effective Period

In the range of shorter period, the energy spectrum is given by Eq.(2.27). The energy spectrum for the inelastic system is obtained by Eq.(2.26).

Denoting $T_m = T_0 + 2\Delta T$, $T_m$ means the maximum value of the instantaneous period of vibration. Substituting Eq.(2.27) into $V_E$ in Eq.(2.26), $E$ is obtained as

$$E = \frac{M}{2}\left(a\sqrt{\frac{T_0^2+T_0T_m+T_m^2}{3}}\right)^2 = \frac{M(aT_e)^2}{2} \tag{2.32}$$

where $T_e = \sqrt{\dfrac{T_0^2 + T_0 T_m + T_m^2}{3}}$ (2.33)

Eq.(2.32) implies that the energy input in the inelastic system can be expressed by the same expression as Eq.(2.27) by applying the effective period, $T_e$ in place of $T_0$.

As is shown in Fig.2.8, Eq.(2.33) can be approximated by

$$T_e = \frac{T_0 + T_m}{2} \tag{2.34}$$

Eq.(2.34) implies that the effective period can be given by the simple average of the natural period and the instantaneous maximum period. Considering that an energy spectrum can be represented by piecewise-linear relations, it is concluded that Eq.(2.34) can be applied to any shapes of energy spectrum.

### 2.2.6 Application of Effective Period

When the restoring force characteristics are to be described precisely, a standard load-deformation relationship is required. To be standard is identical to be well-definable. The best well-definable load-deformation relationship is the load-deformation relationship under monotonic loading. Thus, the monotonic load-deformation curve is indispensable to describe the restoring force characteristics. In Fig.2.9, a monotonic load deformation curve is schematically shown. Referring to a maximum response, $\bar{\mu}$ and the monotonic load-deformation curve, the instantaneous rigidity of a system, $k_s$ can be defined as follows.

$$k_s = \frac{qQ_Y}{(1+\bar{\mu})\delta_Y} \tag{2.35}$$

where $qQ_Y$ : yield level, associated with $\bar{\mu}$

The period of vibration which corresponds to $k_s$, $T_s$ is defined as follows.

$$T_s = 2\pi\sqrt{\frac{M}{k_s}} = T_0\sqrt{\frac{1+\bar{\mu}}{q}} \tag{2.36}$$

The maximum instantaneous period of vibration, $T_m$ can be evaluated on the basis of $T_s$ and is expressed in a following formula[4].

$$T_m = a_T T_s = a_T T_0\sqrt{\frac{1+\bar{\mu}}{q}} \tag{2.37}$$

where $a_T$ : modifying constant

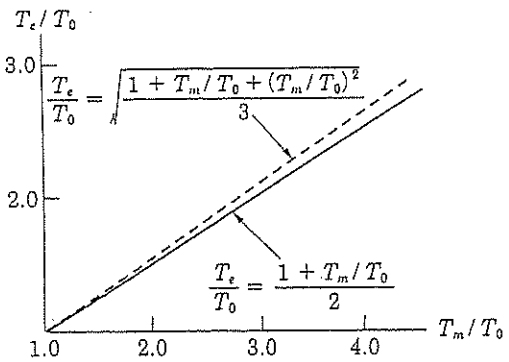


Fig.2.8 Effective Period

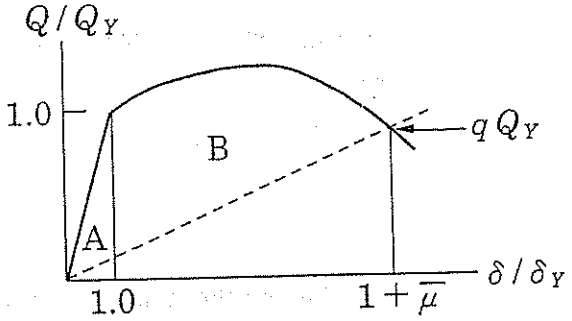


Fig.2.9 Load-Deformation Curve under Monotonic Loading

$a_T$ is obtained as follows, according to the type restoring force characteristics.

For the elastic-perfectly plastic type:

$$a_T = \frac{1+\frac{\bar{\mu}}{8}}{\sqrt{1+\bar{\mu}}} \tag{2.38}$$

For the origin-orienting type and degrading type.

$$a_T = 1.0 \tag{2.39}$$

In Figs.2.8(a2), (b2) and (c2), the energy input in inelastic systems are indicated on the abscissa of $T_e$. It is clearly seen that the energy spectra for the elastic system with the damping of $h = 0.1$ can be representative of all cases of energy inputs of the inelastic systems, irrespective of the level of damage. Thus, the envelope spectrum shown by broken lines can be a design spectrum for general use.

## 3. Energy Input in Multi-Degree of Freedom System [3)]

### 3.1 Energy Input in Elastic System

Based on the modal analysis, the total energy input in the continuous shear strut shown in Fig.3.1 which corresponds to a system with infinitely large number of masses is given by

$$E = \sum E_j$$

$$E_j = -\int_0^{t_0} \ddot{z}_0 \dot{q}_j \left( \int_0^H m \phi_j dx \right) dt \tag{3.1}$$

where $E_j$ : total energy input in $j$th mode

$q_j$ : time function

$\phi_j$ : mode function

$m$ : distributed mass

$H$ : height of shear strut

$x$ : height from the ground

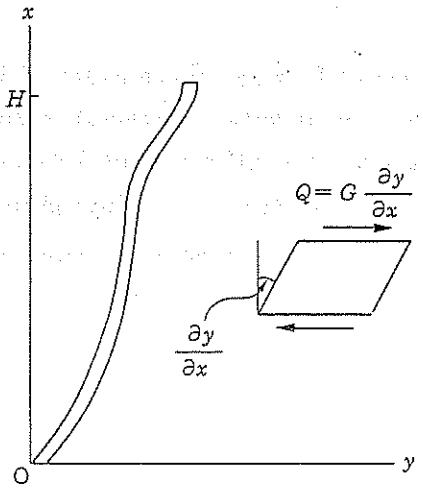


Fig.3.1 Shear Strut

Evaluating $q_j$ and $\phi_j$ for various distribution of shear rigidity, the total energy input was found to be [1)]

$$E > \frac{Mg^2T^2}{4\pi^2} \cdot \frac{\alpha^2(0)}{2} \tag{3.2}$$

where $\alpha(0)$ : base-shear coefficient $= Q_{max}(0)/Mg$

$Q_{max}(0)$ : maximum shear force response at the base

$M$ : total mass

$T$ : fundamental natural period

Therefore, the total energy input in the lastic system can be estimated conservatively by

$$E = \frac{Mg^2T^2}{4\pi^2} \cdot \frac{\alpha^2(0)}{2} \tag{3.3}$$

The base-shear coefficient of structure, $\alpha(0)$ is governed by the fundamental natural period. Then, it can be said that the total energy input in elastic system is only governed by the total mass and the fundamental natural period of the system.

### 3.2 Energy Input in Inelastic System

It is shown that the total energy input in elastic systems is determined exclusively by the total mass and the fundamental natural period. The correspondence between many-mass inelastic systems and many-mass elastic systems is similar to that between one-mass inelastic systems and one-mass elastic systems. That is, plastification has the effect of expanding instantaneous periods. Eventually, the total energy input of an inelastic system governed by the natural period in the elastic range, $T_0$, and a period, $T_1$ greater than that in the elastic range is expressed by a mean value of energy inputs for an elastic system, the natural period of which drops in the range of $T_0 \leq T \leq T_1$. $T_1$ depends on the extent of plastification, becoming longer as plastification develops. In this chapter, the above-mentioned inference will be verified with some specific examples of multi-story inelastic systems. The multi-mass systems adopted are undamped, shear-type five-mass systems.

Because any modes higher than the fifth mode are of no significance in actual buildings, the five-mass system may represent multi-mass systems. A multi-mass vibrational system is specified by the mass ratio $m_i/m_1$, the yield-shear force ratio $\alpha_i/\alpha_1$, the stiffness ratio $k_i/k_1$, and a set of $m_1$, $\alpha_1$, $k_1$. $m_1$ and $k_1$ are reduced to one parameter $m_1/k_1$, as $m_1/k_1$ is related to the fundamental natural period. The subscript, $i$, denoting the number of masses or stories, increases in ascending order with the height of a structure. The yield-shear coefficient, $\alpha_i$ is defined by the following relation.

$$\alpha_i = \frac{Q_{Y_i}}{\sum_{j=i}^{5} m_j g} \tag{3.4}$$

where $Q_{Y_i}$ : yield-shear force coefficient of the $i$th story.

In order to distinguish distributions of parameters, such notations as $M_n$ for the mass distribution, $A_n$ for the yield-shear force distribution, and $K_n$ for the stiffness distribution, are introduced. Thus, a vibrational system is denoted by $M_n$, $A_n$, $K_n$, $\alpha_1$, and $T$.

Table 3.1 Parameters in Vibrational Systems

| | | $i$ (Number of Stories or Masses) | | | | |
|---|---|---|---|---|---|---|
| | Index | 1 | 2 | 3 | 4 | 5 |
| $\frac{m_i}{m_1}$ | $M_1$ | 1.0 | 1.0 | 1.0 | 1.0 | 1.0 |
| | $M_2$ | 1.0 | 0.333 | 0.333 | 0.333 | 0.333 |
| | $M_3$ | 1.0 | 1.0 | 3.0 | 1.0 | 1.0 |
| | $M_4$ | 1.0 | 1.0 | 1.0 | 1.0 | 3.0 |
| $\frac{\alpha_i}{\alpha_1}$ | $A_1$ | 1.0 | 1.10 | 1.25 | 1.565 | 2.0 |
| | $A_2$ | 1.0 | 10.0 | 10.0 | 10.0 | 10.0 |
| | $A_3$ | 1.0 | 10.0 | 10.0 | 10.0 | 1.0 |
| | $A_4$ | 1.0 | 1.0 | 1.0 | 1.0 | 0.1 |
| $\frac{\kappa_i}{\kappa_1}$ | $K_1$ | 1.0 | 0.867 | 0.733 | 0.600 | 0.400 |
| | $K_2$ | 1.0 | 0.820 | 0.640 | 0.500 | 0.200 |
| | $K_3$ | 1.0 | 1.0 | 1.0 | 1.0 | 0.1 |

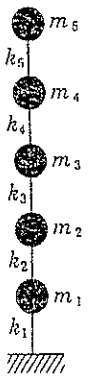

$M_1$ stands for the case of a uniform distribution of masses. $M_2$ expresses the case for which masses other than the first mass are one-third of the first mass. $M_3$ and $M_4$ correspond to the case in which one mass is greater than the others by three times.

$A_1$ expresses the case for which the yield-shear force distribution is controlled so that the cumulated ductility ratio, $\eta_i$, becomes nearly equal in all stories. $\eta_i$ is defined by the accumulated inelastic horizontal deformation of the $i$th story divided by the elastic horizontal deformation of the $i$th story under a yield-shear force. The yield-shear force distribution for this case is obtained by a trial-and-error procedure of numerical analysis. $A_2$ stands for the case in which all the stories above the first story are ten times stronger than the first story. In this case, inelastic deformation can take place only in the first story. $A_3$ is the case for which only first and fifth stories are forced to succumb to inelastic deformation. In the case of $A_4$, only the fifth story behaves inelastically.

$K_1$ and $K_2$ are cases for which spring constants change linearly along the height, $K_2$ being equipped with a steeper change of stiffness distribution. In the case of $K_3$, the stiffness of the fifth story is one-tenth that of the other stories.

Actual buildings are conditioned almost by a set of cases $(M_n, A_n, K_n)$ or $(M_1, A_1, K_1)$. The applied restoring-force characteristics of each story are two typical types. One is the elastic-perfectly plastic type, in terms of story shear-force, $Q_i$, and story displacement, $\delta_i (= y_i - y_{i-1})$ ($y_i$ being a horizontal displacement of the $i$th mass). Another type is the degrading type, as shown in Fig.3.2. Broken lines in this figure, denoted by OAE and OA′E′, are the $Q_i - \delta_i$ relations under monotonic loading in the positive and negative directions, respectively. OAE and OA′E′ are symmetric with respect to the origin, and under an arbitrary history of deformations it is assumed that the $Q_i - \delta_i$ relation is governed by the following law:

The slope in the elastic range is unchangeable, and the slope in the inelastic range, $dQ_i/d\delta_i$ is constant. A relation, which is obtained by connecting through parallel movement, piecewise load-deformation curve in the inelastic range under the positive sign of $Q_i$, coincides with the load-deformation curve under the same sign of monotonic loading. That is, moving parallel

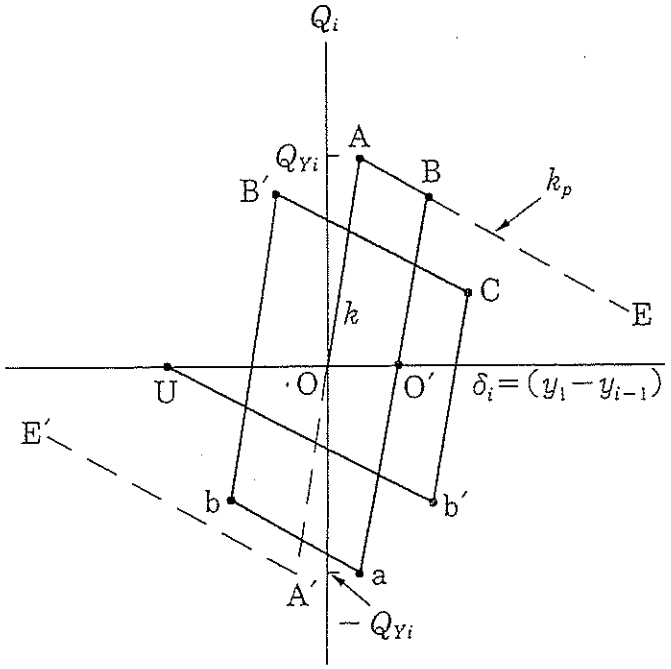


Fig.3.2 Restoring-Force Characteristics with Deterioration in Strength

to the segment B′C in Fig.3.2 and overlapping the point B′ on B, the curve thus obtained, A−B(B′)−C, agrees with the curve under monotonic loading. In the same manner, under the negative sign for $Q_i$, inelastic deformation increments connected sequentially provide the inelastic portion of the monotonic load deformation curve.

Under such a hysteretic law, inelastic deformation develops until point U in Fig.3.2 is reached, where with $Q_i = 0$, the restoring force is lost, and the system loses its resistance to the $P-\delta$ effect (due to vertical loading) and collapses. The aim of applying such degrading types of restoring-force characteristics is to discern whether the energy input in a system that collapses in a certain story is comparable to that in a system with elastic-perfectly plastic restoring-force characteristics. The accelerogram used is from El Centro.

Total energy input can be calculated by the following equation, using a velocity for each mass, $\dot{y}_i$, relative to the ground.

$$E = -\sum_{i=1}^{5}\left(m_i \int_0^{t_0} \ddot{z}_0 \dot{y}_i \, dt\right) \tag{3.5}$$

In Fig.3.3, the relation between the non-dimensionalized total energy input, $A_E$ and $\alpha_1$ is shown for a representative natural period.

$A_E$ is defined to be

$$A_E = E/\frac{Mg^2 T^2}{4\pi^2} \tag{3.6}$$

The solid line in the figure is the total energy input of undamped one-mass systems with restoring-force characteristics of the elastic-perfectly plastic type. It is clearly shown in the figure that the energy input into five-mass systems is fairly close to that in one-mass systems.

Similarly, the energy input in elastic-perfectly plastic systems is shown in Fig.3.4, in which the solid line indicates the responses of one-mass systems. $A_E-\alpha_1$ relations ($A_E-\alpha_5$ in the case of $A_4$ where only the fifth story can behave inelastically) for various sets of $K_n$, $M_n$, and $A_n$ are compared. The aim is to discern the dependence of the total energy input on the stiffness distribution, the mass distribution, and the strength distribution. As a rule, it may be said that the stiffness distribution, the

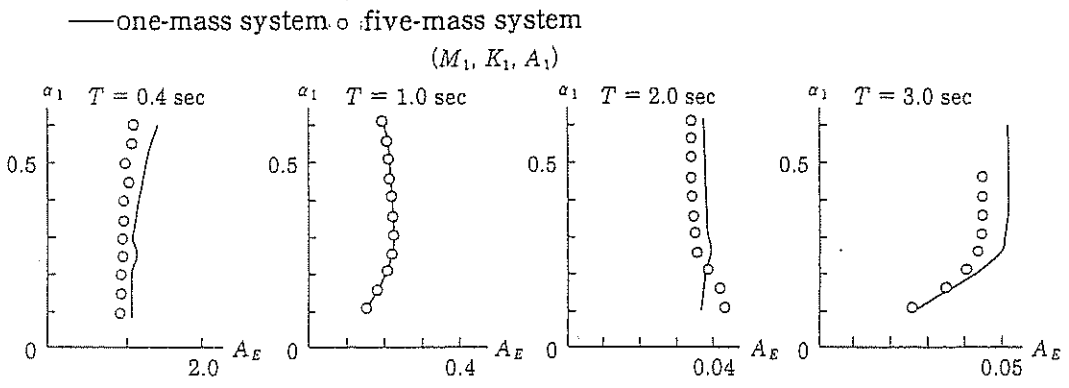


Fig.3.3 Comparison of Energy Input between One-Mass System and Five-Mass System

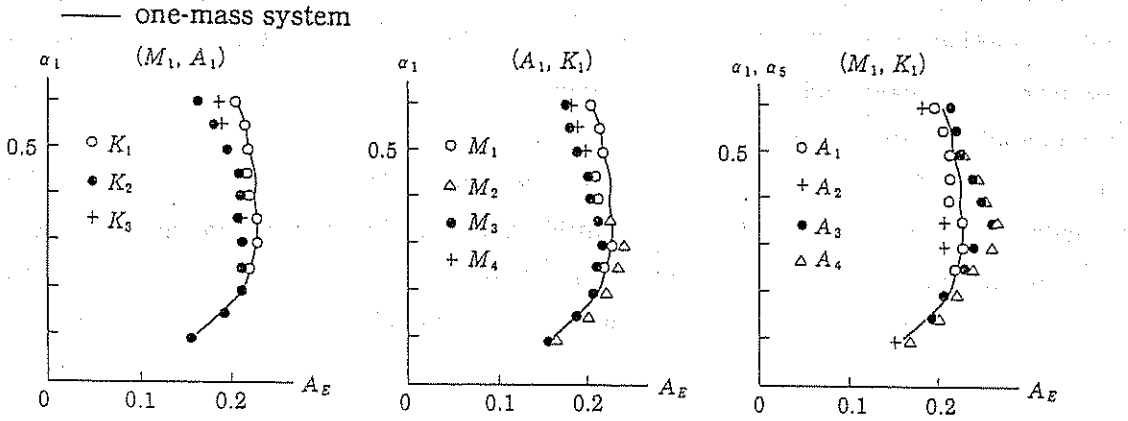


(a) dependence on stiffness distribution

(b) dependence on mass distribution

(c) dependence on strength distribution

Fig.3.4 Energy Input in Five-Mass Systems

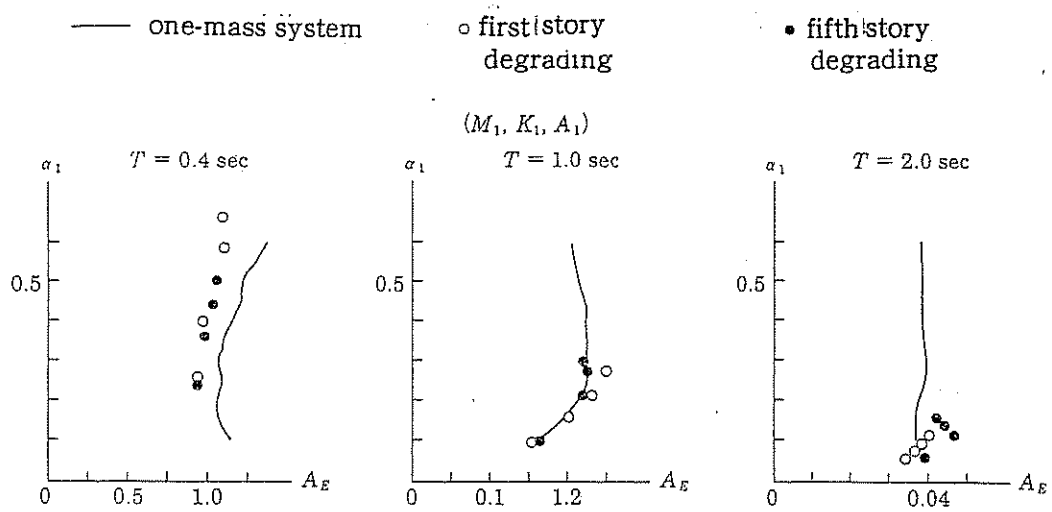


Fig.3.5 Energy Input in Degrading Systems

mass distribution, and the strength distribution are not influential with regard to the total energy input.

Fig.3.5 shows the response of a five-mass system that is equipped with the degrading type of restoring-force characteristics (as shown in Fig.3.2) in the first or fifth story, while the other stories are of the elastic-perfectly plastic type. This case is conditioned by $(M_1, K_1, A_1)$. The ratios of the slope in the degrading range, $k_p$ to that in elastic range, $k$ were selected to be

$$\frac{k_p}{k} = -0.025,\ -0.05,\ -0.075,\ -0.1$$

Whether a story with a degrading type of restoring-force characteristics will collapse depends on the magnitude of the yield-shear force. The magnitude of the yield-shear force for each story is described by $\alpha_1$. It is obvious that the larger $\alpha_1$ becomes, the less the possibility of collapse. When the limit of $\alpha_1$, which enables the system to remain uncollapsed is denoted by $\alpha_m$, collapse does not

occur under the condition $\alpha_m < \alpha_1$, $\alpha_1$, at the collapse limit, is obtained by making $\alpha_1$ increase gradually, and is shown in Fig.3.5. As for the relation between $|k_p|/k$ and $\alpha_m$, a larger value of $\alpha_m$ is required to prevent collapse as $|k_p|/k$ increases, owing to the decrease of inelastic energy absorption capacity in the degraded story.

Four points in the figure, which correspond to each natural period and the position of each degraded story, are located upward from one another, in ascending order of magnitude of $|k_p|/k$. As clearly shown by the figure, even the total energy input in a building which just collapses in a certain story is nearly equal to that of a one-mass system with elastic-perfectly plastic restoring characteristics.

## 4. Estimate of Structural Damage

### 4.1 Expression of Damage

In the basic equation of earthquake resistant design based on the balance of energy shown by Eq(2.10), the term which corresponds to structural damage is $W_p$. Whereas the elastic deformation is restored to the non-stress state as the load is removed, the inelastic deformation remains unreleased and is monotonously accumulated until the collapse state is reached.

In this sense, the cumulated inelastic deformation or cumulated inelastic strain energy can be called damage and its quantity implies the degree of damage. $W_p$ means the total sum of structural damage. When a structure is composed of many elements, $W_p$ is generally written as

$$W_p = \sum W_{pi} \tag{4.1}$$

where $W_{pi}$ : cumulative inelastic strain energy of $i$th element

Assuming a structure with a single element, $W_p$ is expressed as follows.

$$W_p = Q_Y \delta_p = \eta Q_Y \delta_Y \tag{4.2}$$

where $\eta = \dfrac{W_p}{Q_Y \delta_p}$ : cumulative inelastic deformation ratio

$\delta_p$ : cumulative inelastic deformation

$\eta$, being a nondimensionalised damage, is called cumulative inelastic deformation ratio.

Assuming the elastic-perfectly plastic restoring force characteristics, $\eta$ is written as

$$\eta = \frac{\delta_p^+ + \delta_p^-}{\delta_Y} = \eta^+ + \eta^- \tag{4.3}$$

where $\eta^+ = \delta_p^+ / \delta_Y$ : cumulative inelastic deformation ratio in the positive direction (see Fig.4.1)

$\eta^- = \delta_p^- / \delta_Y$ : cumulative inelastic deformation ratio in the negative direction

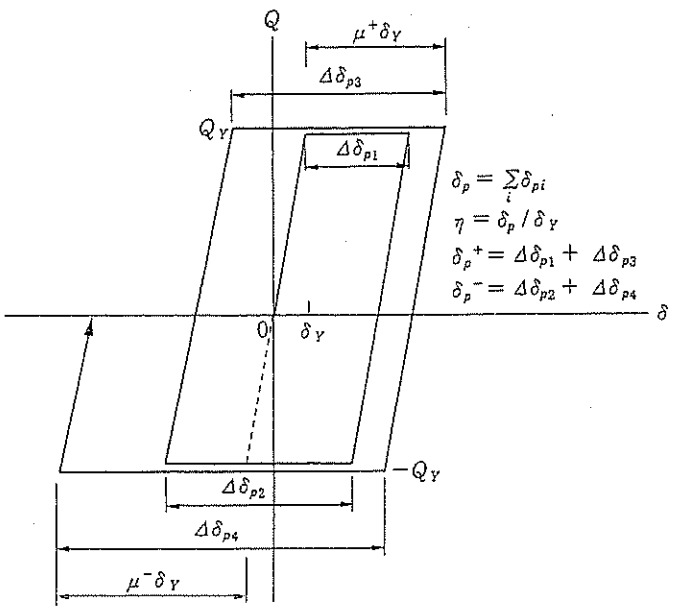


Fig.4.1 Restoring Force Characteristics of Elastic-Perfectly Plastic Type

In this case, $\eta$ means the real cumulative inelastic deformation divided by the elastic limit deformation. A visual image of damage can be given by the residual deformation. The residual deformation in case of the elastic-perfectly plastic restoring force characteristics, $\delta_r$ is expressed by

$$\delta_r = \left|\delta_p^+ - \delta_p^-\right| = \left|\eta^+ - \eta^-\right|\delta_Y \tag{4.4}$$

Another important expression of damage is the maximum deformation or the apparent maximum plastic deformation as stated in 2.2.4.

The apparent maximum plastic deformation can be related to the cumulative plastic deformation. The nondimensionalised apparent maximum plastic deformation is expressed by $\mu$ as shown by Eqs.(2.30) and (2.31). Then, the estimate of $\eta$, $\left|\eta^+ - \eta^-\right|$ and $\mu$ is essential in the seismic design. Among them, $\eta$ can express most directly the structural damage. $\left|\eta^+ - \eta^-\right|$ and $\mu$ can be subsequently qualified in relation to $\mu$.

When $W_p$ is dominant in Eq(2.10), $W_e + W_h$ can be neglected and $\eta$ is quantified based on the following relationship.

$$W_p = E \tag{4.5}$$

When the system consists of single element, $\mu$ can be directly obtained from Eq(4.5).

When the system consists of plural elements, the total damage is clearly described by Eq(4.5). As for the distribution of $W_{pi}$, however, any possibilities can exist. Therefore, it is most important to clarify a law governing the distribution of $W_{pi}$.

### 4.2 Basic Damage Distribution Law Applied to Shear-Type Systems with Elastic-Perfectly Plastic Restoring-Force Characteristics

The yield strength of $i$th story is denoted by $Q_{Yi}$ and the elastic limit deformation under $Q_{Yi}$ is denoted by $\delta_{Yi}$. Using the cumulative inelastic deformation ratio of $i$th story, $\eta_i$, $W_{pi}$ is expressed as

$$W_{pi} = \eta_i Q_{Yi} \delta_{Yi} \tag{4.6}$$

The spring constant of $i$th story is denoted by $k_i$. Using the total mass, $M$ and the fundamental natural period, $T$, the spring constant of an equivalent one-mass system, $k_{eq}$ is define as

$$k_{eq} = \frac{4\pi^2 M}{T^2} \tag{4.7}$$

$k_i$ is related to $k_{eq}$ by the following expression

$$k_i = \kappa_i k_{eq} \tag{4.8}$$

Then, Eq(4.6) is rewritten as

$$W_{pi} = \frac{Mg^2 T^2}{4\pi^2} c_i \alpha_i^2 \eta_i \tag{4.9}$$

$$\text{where} \quad c_i = \left( \frac{\sum_{j=i}^{N} m_j}{M} \right)^2 \frac{1}{\kappa_i} \tag{4.10}$$

As a standard distribution of damage, the damage distribution under an uniform distribution of $\eta_i$ is taken as follows

$$\frac{W_{pk}}{W_p} = \frac{c_k \alpha_k^2}{\sum_{i=1}^{N} c_i \alpha_i^2} \tag{4.11}$$

The yield shear force coefficient distribution which realizes the standard damage distribution is defined to be the optimum yield shear force coefficient distribution and is expressed as

$$\bar{\alpha}_i = \alpha_i / \alpha_1$$

Eq(4.11) is also written as

$$\frac{W_{pk}}{W_p} = \frac{s_k}{\sum s_j} \tag{4.12}$$

$$\text{where} \quad s_i = c_i \kappa_1 \bar{\alpha}_i^2 = \sum_{j=i}^{N} \left(\frac{m_j}{M}\right) \bar{\alpha}_i^2 \left(\frac{k_1}{k_i}\right) \tag{4.13}$$

Eq(4.13) signifies that the standard damage distribution is given by the mass distribution, the spring constant distribution and the optimum yield shear force coefficient distribution.

### 4.3 Optimum Yield Shear Force Coefficient Distribution

If the optimum yield shear force coefficient distribution is unchanged, irrespective of the quantity of $\eta_i$, $\bar{\alpha}_i$ can be given by the shear force coefficient distribution of the elastic system which corresponds to the case of infinitesimally small constant damage.

The above-mentioned inference has been checked to be applied to practical cases, and an unified expression for $\bar{\alpha}_i$ has been already obtained [1].

In Fig.4.2, the optimum yield shear force coefficient distribution which was obtained by a trial-and-error approach applied to multi-mass systems with $N$ of 3 to 9 is shown. The ordinate is taken to be $(i-1)/N$.

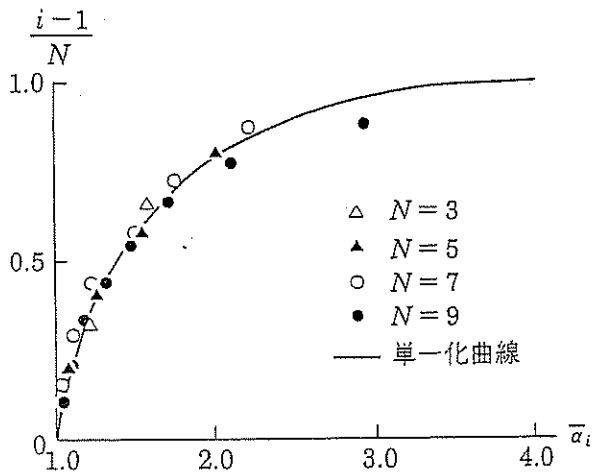


Fig.4.2 Optimum Yield Shear Force Coefficient Distribution

The sequence of the numerical analysis is as follows; First, $\alpha_1$, and $\alpha_i/\alpha_1$ is set, and the response is obtained. A relatively weaker story suffers damage concentration.

Then, in the stories where $\eta_i$ is larger than the averaged damage $\eta_0$, $\alpha_i$ is increased and in the stories where $\eta_i$ is smaller than $\eta_0$, $\alpha_i$ is decreased.

This procedure is repeated several times until the condition of $\eta_i = \eta_0$ is almost satisfied. Used accelerogram is of El Centro (1940). The result of analysis can be expressed by an unified curve as shown in Fig.4.2.

The unified curve is expressed by

$$\left.\begin{aligned} &\text{for} \quad x \geq 0.2, \\ &\quad \bar{\alpha}_i = 1+1.5927x-11.8519x^2+42.5833x^3-59.48272+30.1586x^5 \\ &\text{for} \quad x < 0.2, \\ &\quad \bar{\alpha}_i = 1+0.5x \end{aligned}\right\} \qquad (4.14)$$

$$\text{where} \quad x = \frac{i-1}{N}$$

### 4.4 Damage Distribution Law

#### 4.4.1 Basic Expression

Under the optimum yield shear force coefficient the damage distribution is given by Eq(4.12) Based on numerical analyses for systems equipped with strength distribution different from $\bar{\alpha}_i$, it was found that the damage distribution in general case can be expressed by a following expression continuous to Eq(4.12)

$$\frac{W_{pi}}{W_p} = \frac{s_i p_i^{-n}}{\sum_{j=1}^{N} s_j p_j^{-n}} = \frac{1}{\gamma_i} \qquad (4.15)$$

$$\text{where} \quad p_j = \frac{\alpha_j}{\alpha_1 \bar{\alpha}_j}$$

$n$ : damage concentration index

$\gamma_1$ : damage dispersion factor

$p_j$ expresses the extent of discrepancy of $\alpha_j/\alpha_1$ from the optimum distribution.

When $p_j = 1$, it is obvious that Eq(4.15) is reduced to Eq(4.12). $\gamma_i$ is termed damage dispersion factor, since $\gamma_i$ indicates the extent of damage dispersion into stories other than $i$th story. $n$ is a positive exponent. As $n$ increases, the dependency of damage distribution on $p_j$ increases.

In case of $n = 0$, the damage concentration does not take place. In stories with $p_j > 1$, damage is reduced as $n$ increases. Reversely, in stories with $p_j < 1$, damage concentration is emphasized, as $n$ increases.

#### 4.4.2 Damage Concentration Index

When the damage distribution is given by Eq(4.15), the value of $n$ can be obtained by observing the chance of the damage distribution due to a decrease of strength in the observed story as follows. First, the damage distribution in $k$th story under an arbitrary strength distribution is obtained as

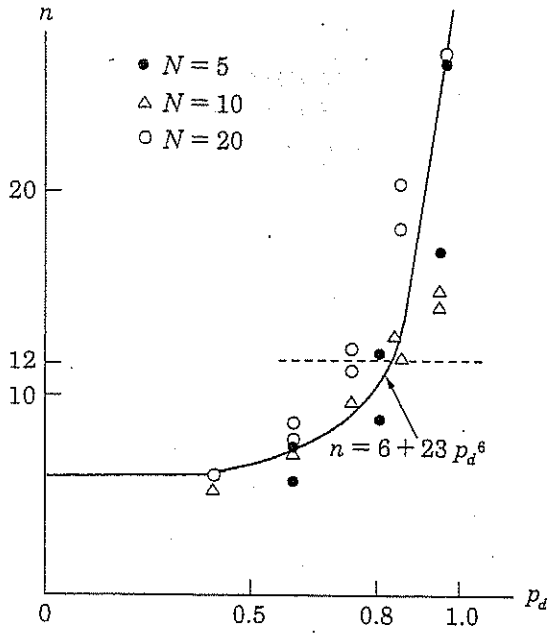


Fig.4.3 Value of $n$ for Weak Column Type of Frames

follows.

$$a = \frac{W_{pk}}{W_p} = \frac{s_k p_k^{-n}}{\sum_{j=1}^{N} s_j p_j^{-n}} \tag{4.16}$$

Next, the damage distribution under another strength distribution in which the strength in $k$th story is modified by multiplying $p_d$ is obtained as follows.

$$b = \frac{W_{pk}}{W_p} = \frac{s_k p_k^{-n} p_d^{-n}}{\sum_{j \neq k} s_j p_j^{-n} + s_k p_k^{-n} p_d^{-n}} \tag{4.17}$$

From Eqs.(4.16) and (4.17), the value of $n$ is obtained as follows

$$n = -\ell_n \left\{ \frac{b(1-a)}{a(1-b)} \right\} \Big/ \ell_n p_d \tag{4.18}$$

Herewith, the result of analysis is shown. Fig.4.3 shows the value of $n$ for weak-column type of frames with elastic-perfectly plastic restoring force characteristics. It is obvious that $n$ can be expressed by an increasing function of $p_d$. It is already ascertained that the value of $n$ for the weak-column type of frames should be 12[1].

$n = 12$ corresponds to an upper bound value for $p_d = 0.8$. Then, it can be deduced that the value of $n$ for practical use can be obtained by taking $p_d = 0.8$ in Eq(4.18)

In Fig.4.4, the value of $n$ for weak-beam type of frames is shown, taking $p_d = 0.8$ and varying stiffness ratios between columns and beams, $k_{cb}$.

$k_{cb}$ is the ratio of stiffness of column to stiffness of beam. A reasonable result that the damage concentration is mitigated by the increase of stiffness of column is clearly seen in decreasing tendency

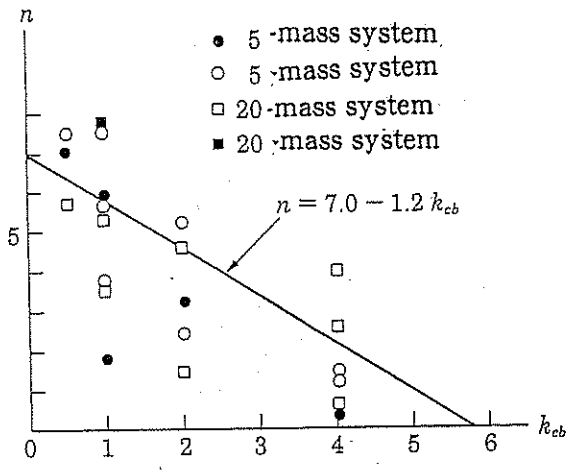


Fig.4.4 Value of $n$ for Weak Beam Type of Frames

of $n$ as $k_{cb}$ increases.

As a representative and conservative value of $n$ for the weak-beam type frames, $n = 6$ can be taken.

### 4.5 Relationship between Cumulative Inelastic Deformation and Maximum Deformation

A load-deformation relationship under a monotonic loading is indicated in Fig.4.5, in which $Q_Y$ is the yield strength and $\delta_Y$ is the elastic deformation corresponding to $Q_Y$.

The inelastic strain energy under the monotonic load-deformation curve, $W_{pm}$ is defined to be

$$W_{pm} = \int_{\delta_Y}^{\delta_m} Q\, d\delta \tag{4.19}$$

Using the inelastic deformation ratio, $\mu$,

$\delta_m$ is written as

$$\delta_m = (1+\mu)\delta_Y \tag{4.20}$$

$W_{pm}$ is an increasing function of $\mu$.

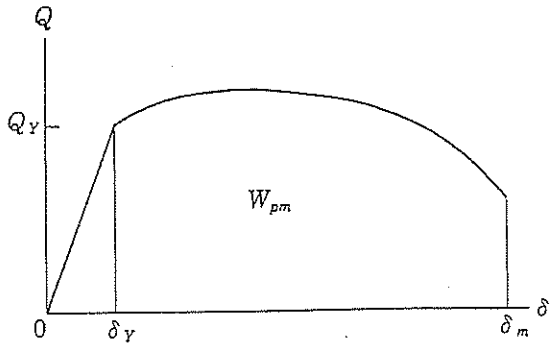


Fig.4.5 Load-Deformation Curve under Monotonic Loading

Under a seismic excitation, a structure develops maximum deformations in positive and negative directions, $\delta^+$, $\delta^-$. $\mu^+$ and $\mu^-$ correspond to $\delta^+$ and $\delta^-$, and $\bar{\mu}$ is the average of $\mu^+$ and $\mu^-$.
The cumulative strain energy of a story can be formally expressed as follows, using $W_{pm}$ given by Eq(4.19).

$$W_p = 2W_{pm}(\bar{\mu})a_p \tag{4.21}$$

$a_p$ is a coefficient and is defined to be

$$a_p = \frac{W_p}{2W_{pm}(\bar{\mu})} \tag{4.22}$$

The cumulative inelastic deformation ratios, $\eta^+$ and $\eta^-$ are defied to be

$$\eta^+ = \frac{W_p^+}{Q_Y\delta_Y},\ \eta^- = \frac{W_p^-}{Q_Y\delta_Y} \tag{4.23}$$

where $W_p^+$, $W_p^-$ : cumulative inelastic strain energy in positive and negative loading domain

The sum of $\eta^+$ and $\eta^-$ is the cumulative inelastic deformation ratio, $\eta$ and the average of $\eta^+$ and $\eta^-$ is the mean cumulative inelastic deformation ratio, $\bar{\eta}$.
A non-dimensional expression of $W_{pm}$ is defined by

$$A_{pm}(\bar{\mu}) = \frac{W_{pm}(\bar{\mu})}{Q_Y\delta_Y} \tag{4.24}$$

Using these quantities and referring to Eq(4.21), the following equation is obtained.

$$\bar{\eta} = A_{pm}(\bar{\mu})a_p = \frac{A_{pm}(\bar{\mu})}{\bar{\mu}}a_p\bar{\mu} \tag{4.25}$$

Referring to Eq(4.25), the following expression is obtained.

$$\frac{\bar{\eta}}{\bar{\mu}} = \frac{A_{pm}(\bar{\mu})}{\bar{\mu}}a_p \tag{4.26}$$

The greater of $\eta^+$ and $\eta^-$ is defined to be $\mu_m$. Then, knowing $\eta = 2\bar{\eta}$, the next equation holds.

$$\frac{\eta}{\mu_w} = \frac{2A_{pm}(\bar{\mu})a_p}{\bar{\mu}}\cdot\frac{\bar{\mu}}{\mu_m} \tag{4.27}$$

$\bar{\mu}/\mu_m$ expresses the deviation of maximum deformations in one direction, being in the range of

$$0.5 \le \frac{\bar{\mu}}{\mu_m} \le 1.0 \tag{4.28}$$

Referring to Eq(4.27), the following relationship is obtained.

$$\frac{A_{pm}}{\bar{\mu}}a_p \le \frac{\eta}{\mu_m} \le 2.0\frac{A_{pm}}{\bar{\mu}}a_p \tag{4.29}$$

When the monotonic load-deformation curve is elastic-perfectly plastic type, $A_{pm}/\bar{\mu}$ is unify and

Eq(4.29) is reduced to

$$a_p < \frac{\eta}{\bar{\mu}_m} < 2.0\, a_p \tag{4.30}$$

When $a_p$ and $\bar{\mu}/\mu_m$ are quantified, the maximum deformation is related to the cumulative inelastic deformation. Since $\eta$ is definitely related to the total energy input, the maximum deformation is related to the total energy input. In order to obtain $a_p$ and $\bar{\mu}/\mu_m$, the numerical analysis is indispensable.

Using shear type of multi-story frames, $\eta-\mu_m$ relationship is quantified.

A general form of the shear-type frame can be expressed by the flexible-stiff mixed frame. The flexible-stiff mixed frame is characterized by the mixture of the flexible elastic element and the stiff elastic-plastic element in each story as shown in Fig.4.6.

Ordinary structures, which are not intentionally equipped with flexible elements, are identified to be structures singly equipped with stiff element (ordinary structures).

By introducing flexible elements, hysteretic behaviors tend to orient the point of origin.

As a result, the residual deformation is reduced and the maximum deformation is restrained under a certain amount of energy input. The flexible-stiff mixed structure is characterized by the rigidity ratio, $r_k$ and the shear force ratio, $r_q$ defined by

$$r_k = \frac{k_f}{k_s} \tag{4.31}$$

$$r_q = \frac{{}_f\bar{Q}_m}{{}_sQ_Y} \tag{4.32}$$

where $k_f$ : spring constant of flexible element

$k_s$ : spring constant of rigid element

${}_f\bar{Q}_m$ : average of maximum shear forces developed in the positive and negative loading domains in flexible element

${}_sQ_Y$ : yield shear force of rigid element

$\bar{\mu}$ : average inelastic deformation ratio

$r_q$ under a maximum deformation of $\bar{\mu}\,{}_s\delta_Y$ ( ${}_s\delta_Y$ : elastic limit deformation of stiff element) is expressed as follows, knowing

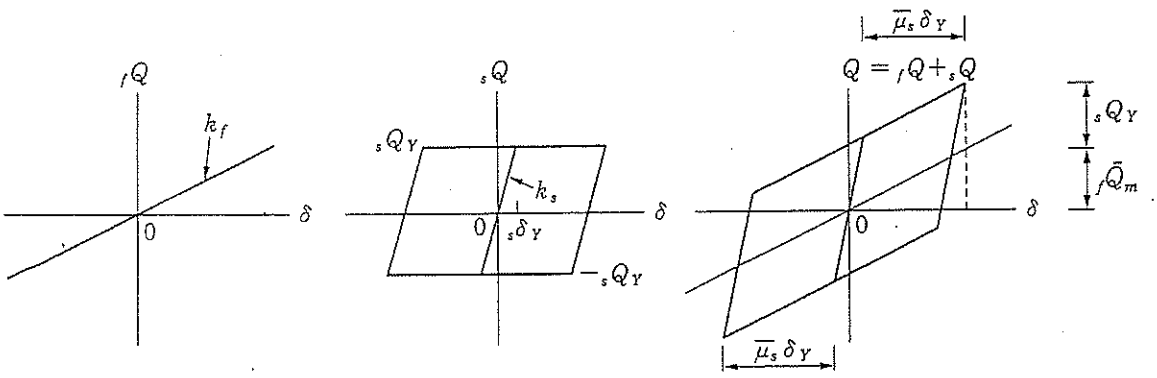


(a) flexible element (b) stiff element (c) mixed system

Fig.4.6 Flexible-Stiff Mixed Structure

$${}_sQ_Y = k_s\delta_Y,\quad {}_f\bar{Q}_m = k_f(1+\bar{\mu})_s\delta_Y.$$

$$r_q = (1+\bar{\mu})r_k \tag{4.33}$$

When $k_f$ and ${}_sQ_Y$ are kept constant values, it is anticipated that as $k_s$ becomes greater, the stiff element absorbs energy more efficiently, thus the maximum deformation being more effectively restrained. However, as $k_s$ becomes greater, $r_k$ is decreased. Therefore, $r_k$ can not be a major quantity effective to restrain the maximum deformation. On the other hand, $r_q$ expresses directly the degree of origin-orienting tendency, thus, can be a major quantity to restrain the maximum deformation. In this context, the results of numerical analysis are arranged by using $r_q$. Used restoring force characteristics are elastic-perfectly plastic type.

In Fig.4.7, deformation responses are shown for three different seismic records.

a) Deviation of Maximum Deformation

In Fig.4.7(a), $\mu_m/\bar{\mu}-r_q$ relationship is shown for $T_f = 2.5$ sec These results are summarized as follows.

Upper bound value:

$$\left.\begin{aligned} &\text{for}\quad r_q \le 1.0,\quad \frac{\mu_m}{\bar{\mu}} = \frac{2+2r_q}{1+2r_q} \\ &\text{for}\quad r_q > 1.0,\quad \frac{\mu_m}{\bar{\mu}} = \frac{4}{3} \end{aligned}\right\} \tag{4.34}$$

Medium value:

$$\left.\begin{aligned} &\text{for}\quad r_q \le 1.0,\quad \frac{\mu_m}{\bar{\mu}} = \frac{3+r_q}{2+2r_q} \\ &\text{for}\quad r_q > 1.0,\quad \frac{\mu_m}{\bar{\mu}} = 1.0 \end{aligned}\right\} \tag{4.35}$$

**b) Deviation of Cumulative Inelastic deformation**

In Fig.4.7(b), $\eta_m/\bar{\eta}-r_q$ relationship is shown for $T_f = 2.5$ sec. As $r_q$ increases, $\eta_m/\bar{\eta}$ rapidly converges to unity. Referring to Eq.(4.4), it can be seen that residual deformation almost vanishes as $r_q$ reaches 0.2.

**c) Correspondence between $\bar{\eta}$ and $\bar{\mu}$**

In Fig.4.7(c), $\bar{\eta}/\bar{\mu}-r_q$ relationship is shown for $T_f = 2.5$ sec. Results are summarized as

Lower bound value:

$$\left.\begin{aligned} &\text{for}\quad r_q \le 1.0,\quad \frac{\bar{\eta}}{\bar{\mu}} = 2+2r_q \\ &\text{for}\quad r_q > 1.0,\quad \frac{\bar{\eta}}{\bar{\mu}} = 4.0 \end{aligned}\right\} \tag{4.36}$$

Design value:

$$\left.\begin{aligned} &\text{for}\quad r_q \le 1.0,\quad \frac{\bar{\eta}}{\bar{\mu}} = 3+r_q \\ &\text{for}\quad r_q > 1.0,\quad \frac{\bar{\eta}}{\bar{\mu}} = 4.0 \end{aligned}\right\} \tag{4.37}$$

The design value means the value which is proposed for practical use in design and is selected to be slightly larger than the lower bound value.

**d) Correspondence between $\eta$ and $\mu_m$**

In Fig.4.7(d), $\eta/\mu_m - \tau_q$ relationship is shown. Knowing $\bar{\eta}/\bar{\mu}$ and $\mu_m/\bar{\mu}$, $\eta/\mu_m$ is given by

$$\frac{\eta}{\mu_m} = \frac{2\bar{\eta}}{\mu_m} = 2\left(\frac{\bar{\eta}}{\bar{\mu}}\right)\left(\frac{\bar{\mu}}{\mu_m}\right) \tag{4.38}$$

Using the lower bound value of $\bar{\eta}/\bar{\mu}$ (Eq.(4.36)) and the upper bound value of $\mu_m/\bar{\mu}$ (Eq.(4.34)), the lower bound value of $\eta/\mu_m$ is obtained as follows.

$$\left.\begin{aligned} &\text{for} \quad \tau_q \leq 1.0, \quad \frac{\eta}{\mu_m} = 2+4\tau_q \\ &\text{for} \quad \tau_q > 1.0, \quad \frac{\eta}{\mu_m} = 6.0 \end{aligned}\right\} \tag{4.39}$$

To take the lower bound value of $\eta/\mu_m$ for practical design purposes seems to be over-conservative. Taking the design value of $\bar{\eta}/\bar{\mu}$ (Eq.(4.37)) and the medium value of $\bar{\mu}/\mu_m$ (Eq.(4.35)), the design value of $\eta/\mu_m$ is obtained as follows.

$$\left.\begin{aligned} &\text{for} \quad \tau_q \leq 1.0, \quad \frac{\eta}{\mu_m} = 4+4\tau_q \\ &\text{for} \quad \tau_q > 1.0, \quad \frac{\eta}{\mu_m} = 8.0 \end{aligned}\right\} \tag{4.40}$$

The obtained formulas can be applicable for different values of $T_f$ than 2.5sec as shown in Fig.4.7.

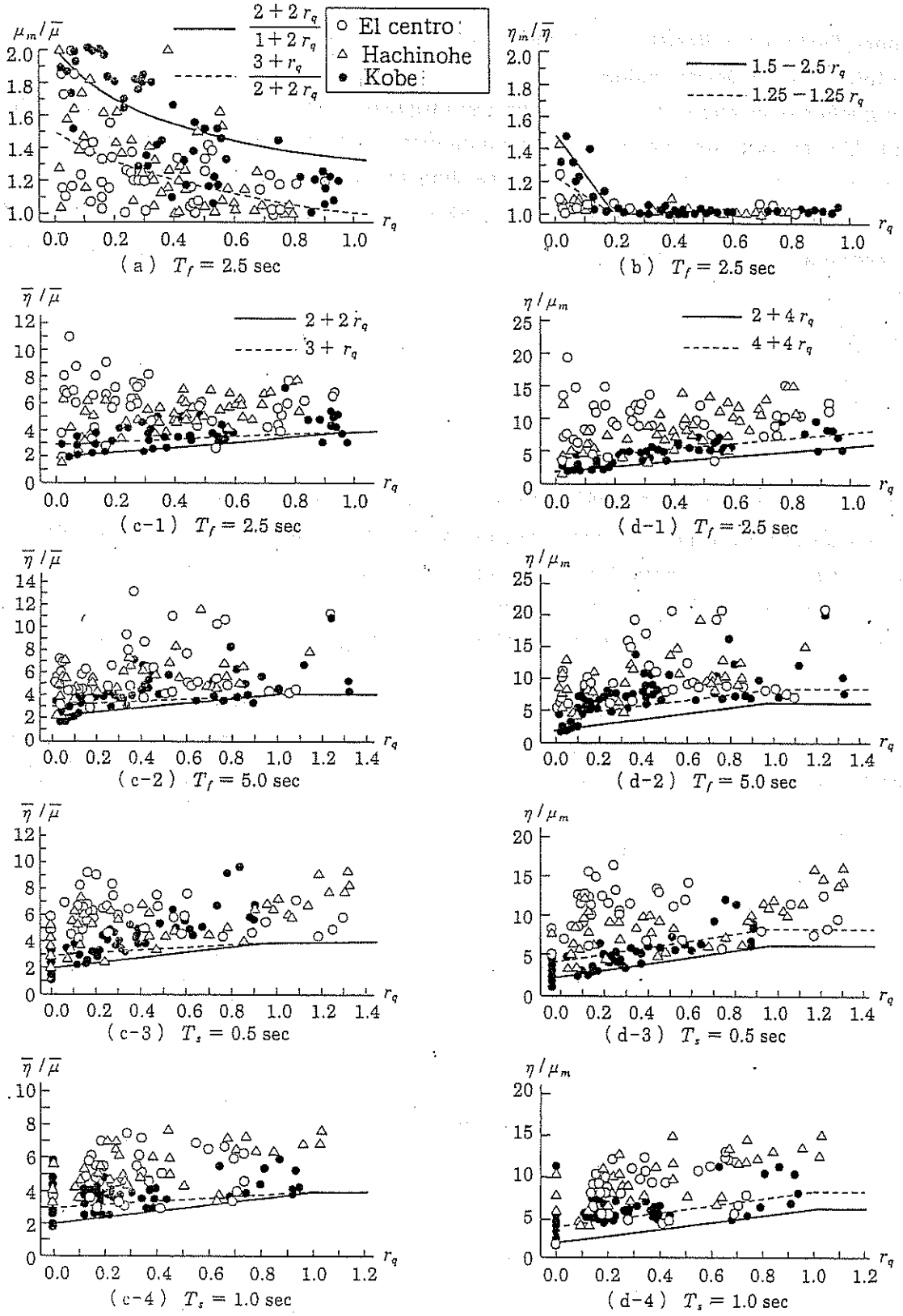


Fig.4.7 Deformation Responses

## 5. Practical application of Energy Approach

### 5.1 Ordinary Earthquake Resistant Structures

#### 5.1.1 Loading Effect of Earthquakes

The loading effect of earthquakes on structures can be grasped most concisely by means of the energy input. The energy input can be expressed in a form of energy spectrum as follows [1].

- The Fourier spectrum of accelerogram of an earthquake motion coincides with the $V_E - T$ relationship of the same earthquake motion. $V_E$ is the equivalent velocity obtained through the following conversion from the total energy input in the undamped one-mass vibrational system with the natural period of $T$.

$$V_E = \sqrt{\frac{2E}{M}} \tag{5.1}$$

where $E$ : total energy input into the system
$M$ : total mass of the system

- The $V_E - T$ relationship defined by Eq.(5.1) is termed as the energy spectrum.
  The energy spectra for damped systems or inelastic systems can be obtained by smoothing (or averaging) the energy spectrum for the undamped elastic system. The extent of smoothing increases proportionally to the extent of nonlinearity of the system.
- The energy spectra for the inelastic systems can be represented by the energy spectrum for the elastic system with 10% of fraction of critical damping ($h = 0.1$). In this sense, it can be easily understood that the total energy input made by an earthquake mainly depends on the total mass and the fundamental natural period of the structure, and is scarcely influenced by the strength, strength distribution, stiffness distribution, mass distribution and type of restoring force characteristics of the structure.

Compared to the conventional acceleration response spectrum and the velocity response spectrum which can be directly applied only to elastic systems, the energy spectrum has decisive advantages as following.

- The energy spectrum can be directly applied both to elastic and inelastic systems.
- The energy spectrum can be represented by a single curve which corresponds to the energy spectrum for the elastic system with $h = 0.1$.
- Two major indices of structural damage are expressed in terms of the cumulative inelastic deformation and the maximum deformation. The cumulative inelastic deformation can be directly related to the total energy input and it is not difficult to find a relationship between the maximum deformation and the cumulative deformation through numerical response analyses.
- On the basis of energy spectrum, the earthquake resistant design can be clearly formulated to be Control of Damage Distribution under a Constant Energy Input.

#### 5.1.2 Earthquake Resistant Design

The equilibrium of energy can be written as

$$W_e + W_h + W_p = E \tag{5.2}$$

where $W_e$ : elastic vibrational energy
$W_h$ : energy absorbed by damping
$W_p$ : cumulative strain energy

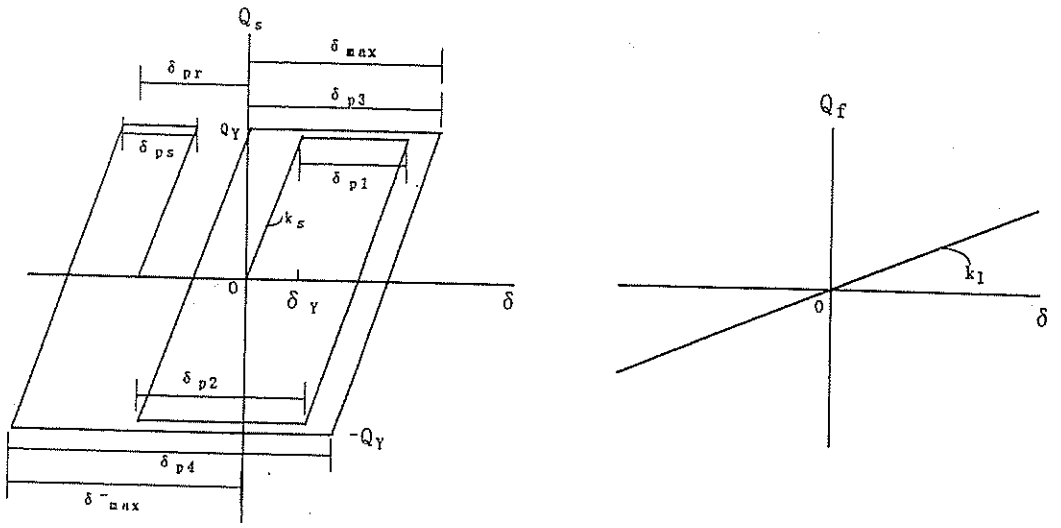


(a) stiff element (b) flexible element

Fig.5.1 Restoring-Force Characteristics

The total energy input $E$ is a very stable amount irrespective of structural behavior.
On the other hand, the distribution of energy over a structure depends on the structural type, and mechanical properties of structural components. The structural damage corresponds to $W_p$.
In order to know the distribution of energy, numerical response analyses are indispensable. By summarizing the results of numerical analyses, it is possible to construct a simplified and conceptual design method based on the energy spectra.

$W_p$ consists of cumulative inelastic strain energy in every story $W_{pi}$. Thus,

$$W_p = \sum_{i=1}^{N} W_{pi} \tag{5.3}$$

where $N$ : number of story.

$W_p$ and $W_{pi}$ can be regarded as structural damage. Each story of a shear type multi-story structures is considered to be composed of a stiff element and a flexible element. The flexible element has a small stiffness and remains elastic, whereas the stiff element has a large stiffness and behaves inelastically. The relation between the shear resistance and the story displacement is depicted in Fig.5.1, where the elastic-perfectly plastic restoring force characteristics of the stiff element is assumed. Assuming that the spring constant of the stiff element, $k_s$ is sufficiently larger than that of the flexible element, $k_f$ and the contribution of energy absorption of the flexible element can be neglected, then, the damage of the first story of a building is written as

$$W_{P1} = \frac{Mg^2T^2}{4\pi^2} \times \frac{2\alpha_1^2\bar{\eta}_1}{\kappa_1} \tag{5.4}$$

where $\alpha_1$ : yield shear force coefficient of the first story ($= Q_{Y1} / Mg$)

$Q_{Y1}$ : yield shear force of the stiff element in the first story

$\bar{\eta}_1$ : averaged comulative inelastic deformation ratio of the stiff element in the first story (=cumulative inelastic deformation / two times of yield displacement)

$\delta_Y$ : yield displacement (see Fig.5.1(a))

$\kappa_1 = k_1/(4\pi^2 M/T^2)$

$g$ : acceleration of gravity

The total damage of a structure. $W_p$ can be formally related to $W_{p1}$ as

$$W_P = \gamma_1 W_{p1} \tag{5.5}$$

In the shear-type multi-story structures, it has been made clear that $\gamma_1$ is expressed by the following formula.

$$\gamma_1 = 1 + \sum_{j \neq 1} s_j (p_j/p_1)^{-n} \tag{5.6}$$

where $p_j = \dfrac{\alpha_j}{\alpha_1 \bar{\alpha}_j}$, $s_j = \left( \sum_{i=j}^{N} m_i/M \right)^2 \bar{\alpha}_j^2 (k_1/k_j)$

$\bar{\alpha}_j$ : optimum yield shear force coefficient distribution

$\alpha_j/\alpha_1$ : actual yield shear force coefficient distribution

$m_i$ : mass of ith floor

$k_i$ : spring constant of ith story

$p_j$ means a deviation of the actual yield shear force distribution from the optimum yield shear force distribution under which the damage of every story $\bar{\eta}_j$ is equalized, and is termed the damage concentration factor. $n$ is termed the damage concentration index. When $n$ becomes sufficiently large, $\gamma_1$ becomes unity. It means that a sheer damage concentration takes place in the first story. When n is nullified, a most preferable damage distribution is realized. Practically, the value of n ranges between 2.0 and 12.0. Weak-column type of structures are very susceptible of damage concentration, and the n-value for them should be 12.0. In weak-beam structures, the damage concentration is considerably mitigated due to the elastic action of columns, and the n-value can be reduced to 6.0. In Fig.5.2 (c), a generalized form of weak-beam type structure is shown. The presence of a vertically extending elastic column is essential to this type of structure. The elastic column by itself is not required to withstand any seismic forces. While ordinary frames pin-connected to the elastic column absorbs inelastically seismic energy, the elastic column plays a role of damage distributor.

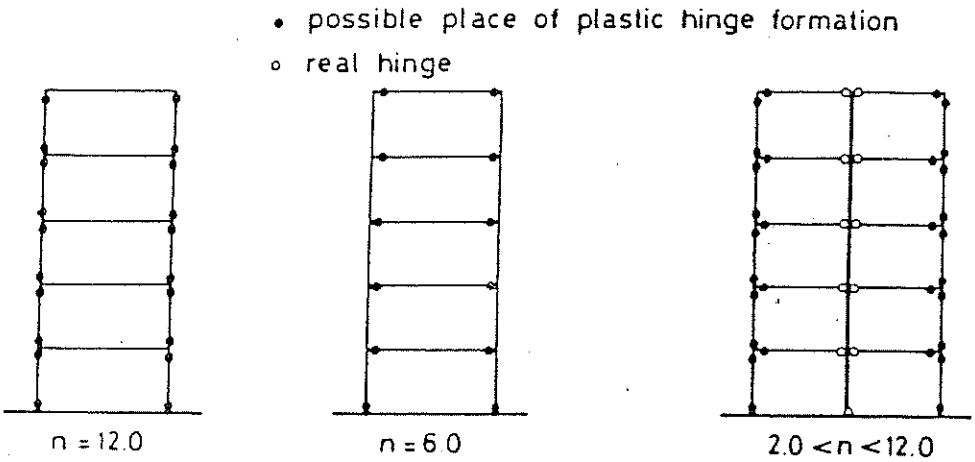


(a) weak-column type (b) weak-beam type (c) generalized weak-beam type

Fig.5.2 Various Structural Types

By applying this type of structure, the n-value can be reduced to 2.0.
The damage concentration is also governed by the value of $p_j$. To simply estimate the damage concentration in the first story, an unified value may be applied as $p_j$ as follows.

$$p_1 = 1.0 \qquad p_{j\neq 1} = p_d \tag{5.7}$$

Eq.(5.7) signifies that the strength gap is assumed between the first story and the other stories. It is impossible to make the yield shear force distribution of an actual multi-story building agree completely with the optimum distribution. The reasons are easily found in the scatter in mechanical properties of material and the rearrangement of geometrical shapes of structural members for the purpose of simplification in fabricating process. Taking account of such a situation, the following value is proposed as a probable strength gap to be taken into account in the design procedure.

$$p_d = 1.185 - 0.0014N \qquad p_d \geq 1.1 \tag{5.8}$$

The elastic vibrational energy is expressed as follows.

$$W_e = \frac{Mg^2T^2}{4\pi^2} \times \frac{\alpha_1^2}{2} \tag{5.9}$$

Taking account of damping, Eq.(5.2) is reduced to

$$W_p + W_e = E \times \frac{1}{\left(1+3h+1.2\sqrt{h}\right)^2} \tag{5.10}$$

where $h$ = damping constant

Substituting Eqs.(5.9) and (5.5) into Eq.(5.10) and using Eq.(5.4), the following formula is obtained.

$$\alpha_1 = \frac{\alpha_e}{\sqrt{1+4\dfrac{\gamma_1\bar{\eta}_1}{\kappa_1}}} \qquad \alpha_e = \frac{2\pi V_E}{Tg} \cdot \frac{1}{1+3h+1.2\sqrt{h}} \tag{5.11}$$

Eq.(5.11) is rewritten as

$$\alpha_1(T) = D_s(\bar{\eta}_1)\alpha_e(T) \tag{5.12}$$

where $\alpha_e(T)$ : required minimum yield shear force coefficient for the elastic system with the fundamental natural period $T$

$\alpha_1(T)$ : required minimum yield force coefficient of the first story for the inelastic system with $T$

$D_s(\bar{\eta})$ : reduction factor for the yield shear force coefficient, which depends on $\bar{\eta}_1$

The distribution of masses is assumed to be uniform. The yield deformation of every story is also assumed constant. Then, the stiffness distribution $k_i/k_1$ becomes equal to the strength distribution $Q_{Yi} / Q_{Y1}$.
The optimum yield shear force coefficient distribution $\bar{\alpha}_i$ is given by the following formula.

$$\bar{\alpha}_i = f\left(\frac{i-1}{N}\right) \tag{5.13}$$

for $x > 0.2$, $f(x) = 1+1.5927x-11.8519x^2+42.583x^3-59.48x^4+30.16x^5$

for $x \leq 0.2$, $f(x) = 1+0.5x$

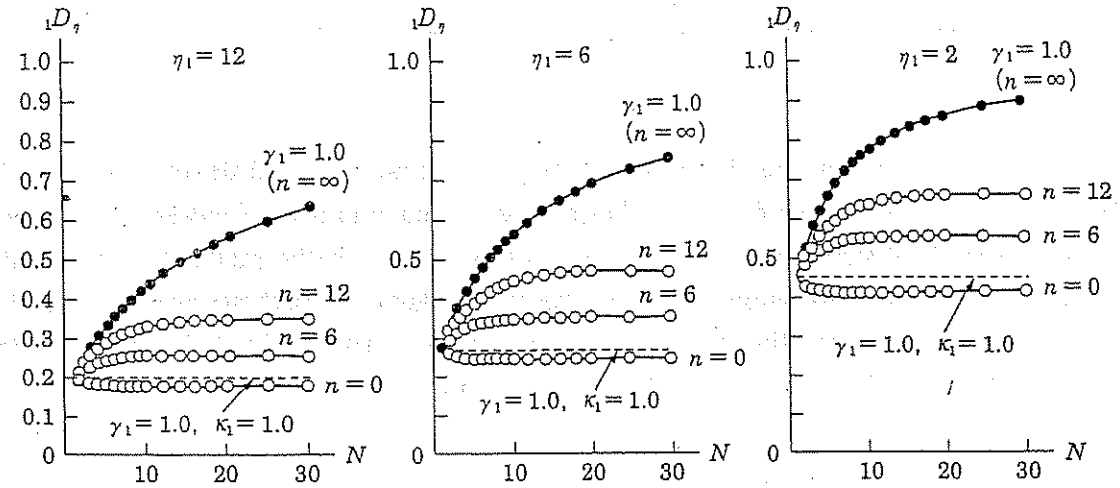


Fig.5.3 $D_s$-Values for Multi-Story Frames

Using the above-mentioned parameters, $\gamma_1$ in Eq.(5.6) and $\kappa_1$ are calculated and approximated by the following relations.

$$\gamma_1 = 1+0.64(N-1)p_d^{-n} \tag{5.14}$$

$$\kappa_1 = 0.48+0.52N \tag{5.15}$$

Then, the $D_s$-value is written as

$$D_s = \frac{1}{\sqrt{1+\dfrac{4\left\{1+0.64(N-1)p_d^{-n}\right\}\bar{\eta}_1}{0.48+0.52N}}} \tag{5.16}$$

Fig.5.3 shows the relationship between the $D_s$-value and the number of story $N$ for specific values of $\bar{\eta}_1$.

The difference of $D_s$-values is caused by the difference of the damage concentration index $n$ which governs the damage distribution in multi-story buildings. $D_s$-values inevitably increase with the increase $N$ due to the effect of damage concentration.

The goal of earthquake resistant design can be summarized as follows.

1) to minimize $\alpha_1$
2) to minimize the maximum story displacement $\delta_{max}$
3) to minimize the residual story displacement $\delta_{pr}$ (see Fig.5.1(a))

To attain the first item, the following two measures are practicable.

1) to increase the deformation capacity $\bar{\eta}_1$
2) to reduce the damage concentration index $n$

The former is realized by applying mild steels to the stiff element. When the structural members are carefully selected so as to avoid structural instability such as local buckling and lateral buckling, it is not impossible to attain the value of $\bar{\eta}_1$ greater than 100. The later is realized by applying the weak-beam type structure or more general damage dispersing systems as shown in Fig.5.2(c).

High-strength steels can be most effectively used as a vertical damage distributor.
To discuss the maximum story displacement, the inelastic deformation ratio, $\bar{\mu}$ is introduced as follows.

$$\bar{\mu} = \left(\bar{\delta}_{max} - \delta_Y\right) / \delta_Y \tag{5.17}$$

where $\bar{\delta}_{max}$ : average value of the maximum story displacement in the positive and negative directions.

The residual story displacement, $\bar{\delta}_r$ is equal to the difference between the cumulative inelastic deformations of positive and negative directions as seen in Fig.5.1(a). To reduce $\bar{\delta}_r$ and $\bar{\mu}$, the most effective measure is the application of "the flexible-stiff mixed structure". Only slight participation of the flexible element enables to nullify $\bar{\delta}_r$ and to reduce $\bar{\mu}$ remarkably as is seen in the following empirical relations (see 4.5).

$$\text{for} \quad \tau_q = 0, \ \bar{\mu} = \frac{\bar{\eta}}{2} \qquad \text{for} \quad \tau_q > 1.0, \ \bar{\mu} = \frac{\bar{\eta}}{4} \qquad \text{to} \quad \bar{\mu} = \frac{\bar{\eta}}{6} \tag{5.18}$$

The stiff elements are the source of energy absorption, whereas flexible elements restrain effectively the development of excessive deformations and one-sided deformations.

## 5.2 BASE-ISOLATED STRUCTURES

In the light of earthquake resistant design method described in the foregoing section, characteristics of base-isolation technique can be summarized as follows.

- Since, by applying flexible isolators at the base of structure, the superstructure can be assumed to be relatively rigid, the base-isolated structure can be assumed to be a single-degree of freedom system under horizontal ground motions
- Since the elastic energy absorption capacity of isolators is large enough to meet the total energy input due to an earthquake, the superstructure is liberated from several restrictions required for ordinary earthquake resistant structures to secure inelastic energy absorption capacity.
- By applying dampers, the horizontal displacement at the base is effectively reduced.

In turn, dampers must absorb almost all of the total energy input. When leads or steels are used for the material of dampers, the restoring-force characteristics at the base of the base-isolated structure take a shape as shown in Fig.5.4. Q denotes the total shear force and $\delta$ denotes the horizontal displacement at the base of base-isolated structure. $\alpha_s$ and $\alpha_f$ are defined as

$$\alpha_s = \frac{{}_sQ_Y}{Mg}, \quad \alpha_f = \frac{{}_fQ_{max}}{Mg} \tag{5.19}$$

where ${}_sQ_Y$ : yield strength of dampers
${}_fQ_{max}$ : maximum shear force of isolators
$M$ : total mass of superstructure

The results of numerical response analysis are summarized as follows.

- The maximum displacement $\delta_{max}$ takes place in almost same amount in the positive and negative directions.

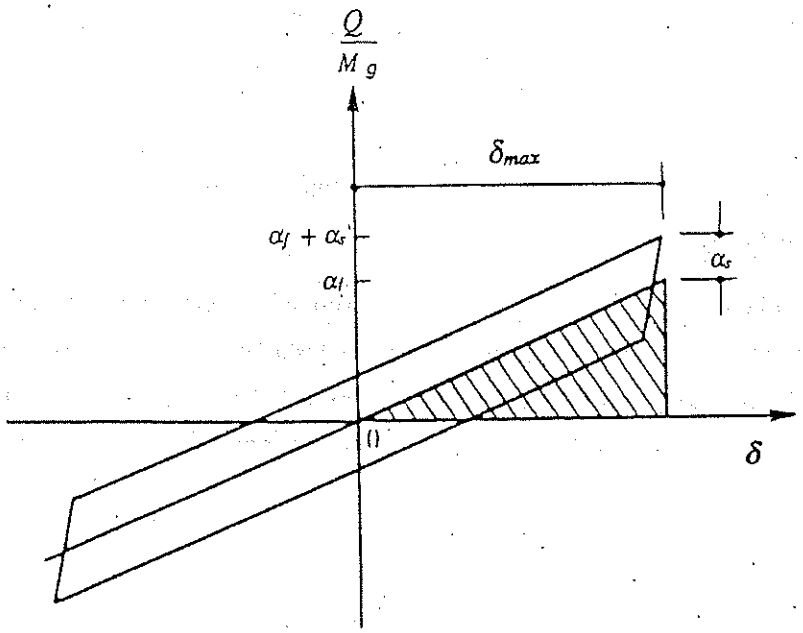


Fig.5.4. Restoring-Force Characteristics of the Base-Isolated Story

- The energy absorbed by dampers at the instant when the maximum displacement is reached can be approximately expressed by the area twice as large as the area covered by the closed loop in Fig.5.4.

The equilibrium of energy at the instant when the maximum displacement is reached can be expressed by

$$W_e + W_p = E(t_m) \tag{5.20}$$

where $W_e$ : energy stored in isolators

$W_p$ : energy stored in dampers

$E(t_m)$ : total energy input at $t = t_m$

$t_m$ : time when the maximum displacement is reached

The energy absorption due to damping of isolators is ignored. Referring the response characteristics, $W_e$ and $W_p$ are written as

$$W_e = \frac{{}_f Q_{max}\,\delta_{max}}{2} \tag{5.21}$$

$$W_p = 8\,{}_s Q_Y\,\delta_{max} \tag{5.22}$$

As the total energy input $E$ is defined to be the energy input exerted by an earthquake during whole duration of time, $E$ is generally greater than $E(t_m)$. Therefore, by applying $E$ in place of $E(t_m)$ in Eq.(5.20), the maximum responses can be obtained with some errors of over-estimate. Then, the basic equation for the estimate of the maximum responses can be written as

$$\frac{{}_f Q_{max}\,\delta_{max}}{2} + 8\,{}_s Q_Y\,\delta_{max} = \frac{M V_E^2}{2} \tag{5.23}$$

$\delta_{max}$ can be expressed as

$$\delta_{max} = \frac{{}_fQ_{max}}{k_f} \tag{5.24}$$

where $k_f$ : spring constant of isolators

$k_f$ is written as

$$k_f = \frac{4\pi^2 M}{T_f^2} \tag{5.25}$$

where $T_f$ : period of base-isolated structure without dampers

Using Eqs(5.19), (5.24) and (5.25), Eq.(5.23) is reduced to

$$\frac{\alpha_f}{\alpha_0} = -a + \sqrt{a^2+1} \tag{5.26}$$

where $a = 8\left(\frac{\alpha_s}{\alpha_0}\right)$

$$a_0 = \frac{2\pi V_E}{T_f g}$$

$\alpha_0$ signifies the shear force coefficient for the base-isolated structure without dampers. The total shear force coefficient at the base of base-isolated structure $\alpha$ is obtained as

$$\alpha = \alpha_f + \alpha_s = \left(-\frac{7a}{8} + \sqrt{a^2+1}\right)\alpha_0 \tag{5.27}$$

Then, the $D_s$-value for the base-isolated structure is obtained as

$$D_s = -\frac{7a}{8} + \sqrt{a^2+1} \tag{5.28}$$

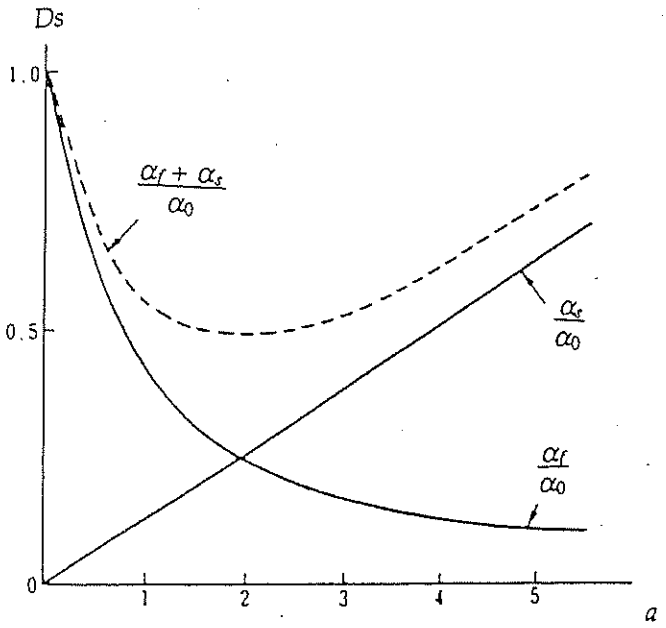


Fig.5.5 Ds-Values for Base-Isolated Structure

The maximum displacement is obtained as

$$\delta_{max} = \frac{{}_fQ_{max}}{k_f} = \frac{T_f^2 \alpha_f g}{4\pi^2} \tag{5.29}$$

The $D_s$-value given by Eq.(5.28) is shown in Fig.5.5. As is seen in the figure, the $D_s$-value for the base-isolated structure is hardly less than 0.5. The major advantage of base-isolated structure in reducing shear force response must be ascribed to the reduction of $\alpha_0$. Since the $V_E$-value in the range of longer periods can be assumed to be constant, to make $T_f$ large is of primary importance for the reduction of $\alpha_0$. In order to make $T_f$ large, the most effective measure is to reduce the number of isolators and this can be realized by properly evaluating huge compressive load-bearing capacity of isolators.

# 6. Prospect and Lessons

## 6.1 Advanced Design Method (Flexible-Stiff Mixed Structures)

### 6.1.1 Introduction

Previous seismic design methods have been developed with structural safety as the major consideration, while performance in other areas has been neglected, with the following results.

- During the severe earthquakes, structure are inevitably damaged to some extent and sometimes, repair is very expensive.
- Strengthening structures in order to reduce structural damage results in an increased acceleration response, which causes overturning of furniture and equipment. Thus, it causes an interruption of daily activities such as medical treatment and results in the loss of property.

On the other hand, the recently developed base-isolation technique has overcome the above-mentioned difficulties, without deterioration of the performance obtained by using conventional earthquake-resistant design methods.

In this section, an earthquake resistant design method for buildings which meets the requirements for both structural safety and reduction of the acceleration response is discussed.

The proposed design method is consistent to the method applied to base-isolated structures and is developed based on the balance between the seismic energy input and the energy absorption capacity of the structure. Structures in general are very complicated and prediction for exact behavior of them is, sometimes, very difficult. Therefore, in order to develop the performance-based design method, it is also necessary to exploit preferable structural types of which prediction of structural behavior can be explicitly made.

As a preferable structural type, the flexible-stiff mixed structure is introduced. The flexible-stiff mixed structure consists of the flexible elements which remain elastic even under severe earthquakes with a relatively low elastic rigidity and the stiff elements which behave mainly plastically with a relatively high elastic rigidity.

Conventional type of multi-story buildings can be remodeled to be a flexible-stiff mixed structure by definitely allotting a role of the flexible element or the stiff element to each structural element. Major damage indices such as the cumulative plastic deformation, the maximum deformation, the residual deformation and the maximum yield shear force coefficient are clearly related to the level of seismic input.

### 6.1.2 Flexible-Stiff Mixed Structure

The structure which is composed of the flexible elements remained elastic and the stiff elements with a high elastic rigidity and a high plastic deformation capacity is defined as the flexible-stiff mixed structure [1]. In flexible-stiff mixed structures, the yield strengths in positive and negative loading domains, $|Q_Y^+|$ and $|Q_Y^-|$, become different as the deformation develops. Generally, cumulative plastic deformations are liable to concentrate in the element with a relatively weak yield strength. Therefore, a further development of the plastic deformation in a loading domain where plastic deformations have developed with an increase of the yield strength is restrained autonomously in the flexible-stiff mixed structure, thus resulting in equalization of deformations in positive and negative loading domains. Main features in the response characteristics of the flexible-stiff mixed structures are summarized as follows.

1) The cumulative plastic defamations in positive and negative loading domains are nearly equal.
2) The maximum deformation in positive and negative loading domains are nearly equal.
3) Efficiency of the energy adsorption with respect to a maximum deformation is high.
4) The residual deformation can be made considerably small.

Referring to these characteristics, in comparison to the ordinary structures consisting of monotonous elastic-plastic elements, the flexible-stiff mixed structures are considered to be a preferable structural type of which performance in the seismic resistance can be clearly stated.

The cumulative plastic deformation, $\delta_p$, is related to the maximum deformation, $\delta_m$, by the following empirical equation in the flexible-stiff mixed structure, neglecting the elastic deformation of the rigid element.

$$\delta_p = 8\delta_m \tag{6.1}$$

Also, the residual deformation in the flexible-stiff mixed structure, $\delta_r$, is expressed empirically as

$$\delta_r = 0.2\,{}_sQ_Y\left(\frac{1}{{}_fk}-\frac{1}{{}_sk}\right), \text{ and also } \delta_r < \delta_m \tag{6.2}$$

where ${}_sQ_Y$ : yield strength of the rigid element

${}_fk$ : rigidity of the flexible element

${}_sk$ : rigidity of the stiff element

### 6.1.3 Response of the Flexible-Stiff Mixed Structure

The form of the energy spectrum can be represented by a bilinear curve shown in Fig.6.1. That is, the $V_E$–$T$ relationship is expressed by a line passing through the point of origin in the short-period range and takes a constant value in the long-period range as is expressed by

$$\text{for } T \le T_G, \quad V_E = \frac{V_{Em}}{T_G}\,T \tag{6.3}$$

$$\text{for } T > T_G, \quad V_E = V_{Em}$$

where $V_{Em}$ : maximum value of $V_E$

The energy input attributable to the structural damage, $E_D$, is also converted to the equivalent velocity, $V_D$, through the equation similar to Eq.(5.1).

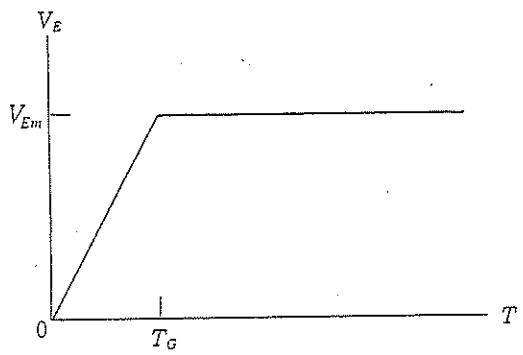


Fig.6.1 Energy Spectrum

$V_D$ is related to $V_E$ by the following empirical formula.

$$V_D = \frac{V_E}{1+3h+1.2\sqrt{h}} \tag{6.4}$$

The flexible-stiff mixed structure is assumed to be a shear type of multistory frame. The restoring force characteristics of the stiff element in each story is assumed to be elastic-perfectly plastic type. A hysteretic behavior of one story is shown in Fig.6.2. The rigidity of the stiff element is denoted by ${}_sk$ and the rigidity of the flexible element is denoted by ${}_fk$. ${}_s\delta_Y$ is the yield deformation of the stiff element. Under the maximum deformation, $\delta_m$ the instantaneous period of vibration of the system takes a value of $T_m$. The secant rigidity, $k_e$, associated with $\delta_m$ can be applied in order to predict $T_m$ by using the following formula.

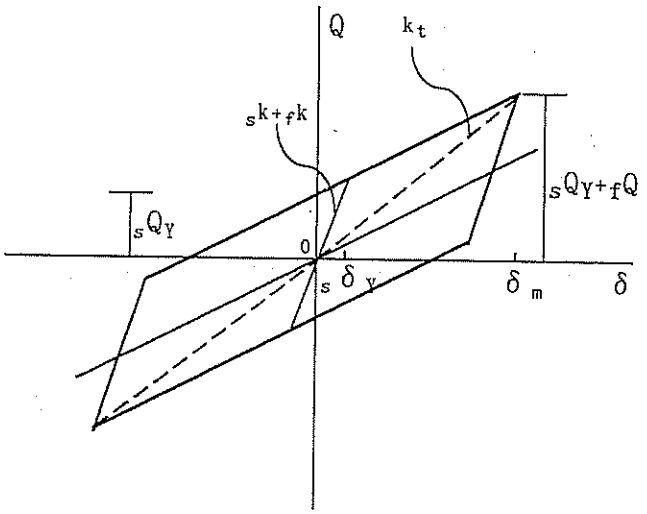


Fig.6.2 Hysteresis Loop

$$T_m = 2\pi\sqrt{\frac{M}{k_e}} \tag{6.5}$$

The energy attributable to the damage can be expressed in terms of potential energy under the gravity field i.e., by the equivalent height of the mass, $h_E$, according to the following equation.

$$h_E = \frac{E_D}{Mg} = \frac{V_D^2}{2g} \tag{6.6}$$

where $g$ : acceleration of gravity

Generally, the energy input attributable to the damage is finally absorbed by structural skeletons of a structure in a form of cumulative plastic deformation. Therefore, the following equation holds.

$$E_D = \sum_{i=1}^{N} W_{pi} \tag{6.7}$$

where $W_{pi}$ : cumulative plastic strain energy in each story

$N$ : number of the story

Eq.(6.7) can be written in respect to the damage of the first story as

$$E_D = W_{p1}\gamma_1 \tag{6.8}$$

where $\gamma_1$ : the ratio of the total damage to $W_{p1}$, given by Eq.(5.14)

The damage concentration index, $n$ is taken to be 6.0 for the flexible-stiff mixed structure.
By dividing Eq.(6.8) with $Mg$, the following equation is obtained.

$$h_E = {}_s\alpha_{Y1}\delta_{p1}\gamma_1 \tag{6.9}$$

where ${}_s\alpha_{Y1} = {}_sQ_{Y1}/Mg$ : yield shear force coefficient in the first story

Using Eqs.(6.1) and (6.9), ${}_s\alpha_{Y1}$ is determined as

$${}_s\alpha_{Y1} = \frac{h_E}{8\gamma_1\delta_{m1}} \tag{6.10}$$

where $\delta_{m1}$ : maximum displacement of the first story

The fundamental natural period of the shear-type system can be written in terms of the spring constant of the first story, $k_1$, as

$$T = 2\pi\sqrt{\frac{M\kappa_1}{k_1}} \tag{6.11}$$

where $\kappa_1 = k_1/k_{eq}$

$k_{eq}$ : equivalent spring constant of the single-degree of freedom system with $M$ and $T$

$\kappa_1$ is given by Eq.(5.15).

$$\kappa_1 = 0.48+0.52N \tag{6.12}$$

While in the long-period range, the energy input is given regardless of the value of the period, the energy input in the short-period range depends on the period. Therefore, the period must be precisely estimated.
The substantial period for the sysytem of which the period of vibration changes between $T_0$ and $T_m$ is calculated for the short-period range as

$$T_e = \sqrt{\frac{T_0^2+T_0T_m+T_m^2}{3}} \tag{6.13}$$

where $T_e$ : substantial period of the sysytem

$T_0$ : period in the elastic range

Referring to Fig.6.2, $T_0$ and $T_m$ are written as

$$T_0 = 2\pi\sqrt{\frac{\kappa_1}{g\left(\frac{{}_s\alpha_1}{{}_s\delta_{Y1}}+\frac{{}_f\alpha_1}{\delta_{m1}}\right)}}, \quad T_m = 2\pi\sqrt{\frac{\kappa_1}{g\left(\frac{{}_s\alpha_1+{}_f\alpha_1}{\delta_{m1}}\right)}} \tag{6.14}$$

where ${}_f\alpha_1 = \frac{{}_fk_1\delta_{m1}}{Mg}$ : shear force cocfficient of the flexible element in the first story

### 6.1.4 Illustrative Example

As an illustrative example, the sysytem in which ${}_sk$ is sufficiently greater than ${}_fk$ and ${}_s\delta_Y$ is negligible small, is taken.

Applying these assumptions, $T_0$ becomes nullified, and $T_e$ is reduced to

$$T_e = \frac{2\pi}{\sqrt{3}}\sqrt{\frac{\kappa_1\delta_{m1}}{(1+f)_s\alpha_{Y1}}} \tag{6.15}$$

where $f = {}_f\alpha_1 / {}_s\alpha_{Y1}$

Denoting $h_E$ at $T = T_G$ by $h_{Em}$, $h_E$ in the short-period range characterized by the linear $V_D - T$ relationship is written as

$$h_E = h_{Em}\left(\frac{T_e}{T_G}\right)^2 \tag{6.16}$$

Using Eqs.(6.10)(6.15) and (6.16), ${}_s\alpha_{Y1}$ for the energy input in the short-period range is determined as follows, regardless of $\delta_{m1}$.

$${}_s\alpha_{Y1} = \frac{\pi}{\sqrt{6}\,T_G}\sqrt{\frac{h_{Em}\kappa_1}{(1+f)g\gamma_1}} \tag{6.17}$$

On the other hand. in the long-period range, since $h_E = h_{Em}$, ${}_s\alpha_{Y1}$ is obtained as

$$\alpha_{Y1} = \frac{h_{Em}}{8\gamma_1\delta_{m1}} \tag{6.18}$$

As an illustrative example, the maximum level of the ground motion which competes with the Hyogoken-nanbu earthquake, 1995 is applied, i.e., $T_G$ and $V_{Em}$ in the energy spectrum shown in Fig.6.1 are selected to be

$$\begin{aligned} V_{Em} &= 400cm \\ T_G &= 1.0sec \end{aligned} \tag{6.19}$$

The damping of $h = 0.02$ is assumed. Then, the maximum value of $V_D$, $V_{Dm}$, and $h_E$ become as

$$\begin{aligned} V_{Dm} &= \frac{V_{Em}}{1+3h+1.2\sqrt{h}} = 325\,cm/sec \\ h_{Em} &= 54\,cm \end{aligned} \tag{6.20}$$

As a structural performance, the maximum story dislacement in the first story is assumed to be

$$\delta_{m1} = 5cm,\ 6.67cm,\ 10cm \tag{6.21}$$

A weak-beam type of structure is assumed, that is, in estimating the damage distribution, $n = 6.0$ is taken.

${}_s\alpha_{Y1}$ obtained by Eq.(6.17) is denoted by $({}_s\alpha_{Y1})_{\mathrm{I}}$ and ${}_s\alpha_{Y1}$ obtained by Eq.(6.18) is denoted by $({}_s\alpha_Y)_{\mathrm{II}}$. The smaller of those becomes the real value of ${}_s\alpha_{Y1}$ which corresponds to the given energy spectrum. The larger value of those corresponds to the extended lines of the two line segments of the energy spectrum. The ${}_s\alpha_{Y1} - N$ relationships for $f = 1.0$ are shown in Fig.6.3 in which the solid lines are valid due to the above-mentioned reason.

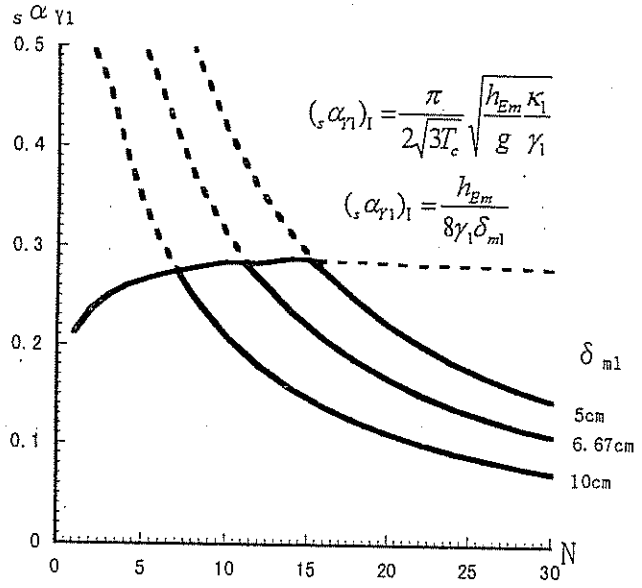


Fig.6.3 ${}_s\alpha_{Y_1}-N$ Relationship

Table 6.1 ${}_s\alpha_{Y_1}-N$ Relationship

| N | $\gamma_1$ | $\kappa_1$ | $(_s\alpha_{Y1})_I$ | $\bar{\delta}_{m1}(cm)$ | $(_s\alpha_{Y1})_{II}$ $\delta_{m1}(cm)$ | | |
|---|---|---|---|---|---|---|---|
| | | | | | 10.0 | 6.67 | 5.0 |
| 1 | 1.00 | 1.00 | 0.213 | 31.7 | 0.675 | 1.011 | 1.350 |
| 2 | 1.23 | 1.52 | 0.237 | 23.2 | 0.548 | 0.822 | 1.096 |
| 3 | 1.47 | 2.04 | 0.251 | 18.3 | 0.459 | 0.688 | 0.918 |
| 4 | 1.71 | 2.56 | 0.261 | 15.1 | 0.394 | 0.591 | 0.788 |
| 5 | 1.96 | 3.08 | 0.267 | 12.9 | 0.344 | 0.516 | 0.688 |
| 6 | 2.21 | 3.60 | 0.272 | 11.2 | 0.305 | 0.458 | 0.610 |
| 8 | 2.71 | 4.64 | 0.279 | 8.9 | 0.249 | 0.373 | 0.498 |
| 10 | 3.23 | 5.68 | 0.285 | 7.4 | 0.209 | 0.313 | 0.418 |
| 12 | 3.77 | 6.72 | 0.284 | 6.3 | 0.179 | 0.268 | 0.358 |
| 14 | 4.32 | 7.76 | 0.289 | 5.5 | 0.156 | 0.234 | 0.312 |
| 16 | 4.89 | 8.80 | 0.286 | 4.8 | 0.138 | 0.207 | 0.276 |
| 18 | 5.47 | 9.84 | 0.286 | 4.3 | 0.123 | 0.185 | 0.247 |
| 20 | 6.07 | 10.88 | 0.285 | 3.9 | 0.111 | 0.167 | 0.222 |
| 22 | 6.68 | 11.92 | 0.283 | 3.6 | 0.101 | 0.151 | 0.202 |
| 24 | 7.32 | 12.96 | 0.283 | 3.25 | 0.092 | 0.138 | 0.184 |
| 26 | 7.97 | 14.00 | 0.282 | 3.0 | 0.085 | 0.127 | 0.169 |
| 28 | 8.64 | 15.04 | 0.281 | 2.8 | 0.078 | 0.117 | 0.156 |
| 30 | 9.32 | 16.08 | 0.280 | 2.6 | 0.072 | 0.109 | 0.145 |

Also, in Table 6.1, the values of ${}_s\alpha_{Y1}$ for $f = 1.0$ are shown. The values of $({}_s\alpha_{Y1})_{II}$ listed above the horizontal line are larger than $({}_s\alpha_{Y1})_I$. Accordingly, those value are not valid. In the short-period range, ${}_s\alpha_{Y1}$ takes a constant value irrespective of $\delta_{m1}$. In this case, however, $\delta_{m1}$ is limited by the condition that $T_e$ does not exceed $T_G$. Denoting $\delta_{m1}$ which corresponds to $T_G$ by $\bar{\delta}_{m1}$, $\bar{\delta}_{m1}$ is written as

$$\bar{\delta}_{m1} = \frac{3g_s\alpha_{Y1}T_G^2}{(1+f)\pi^2\kappa_1} = \frac{\sqrt{3}\,T_G}{2(1+f)\pi}\sqrt{\frac{gh_{Em}}{\kappa_1\gamma_1}} \tag{6.22}$$

In the short period range, an arbitrary value of $\delta_{m1}$ can be taken under a constant value of ${}_s\alpha_{Y1}$. However, under the given condition ${}_f\alpha_{Y1} = f\,{}_s\alpha_{Y1}$, ${}_fk_1$ must be

$${}_fk_1 = \frac{f\,{}_s\alpha_{Y1}}{\delta_{m1}} \tag{6.23}$$

Actually, the restraining condition of Eq.(6.23) can be mitigated, that is, the rigidity higher than that given by Eq.(6.23) can be allowed on the reason that a higher rigidity makes $T_e$ smaller than the prescribed value due to Eq.(6.23), resulting in a decrease of the energy input in the short-period range. In the region of $\delta_{m1} > \bar{\delta}_{m1}$, ${}_s\alpha_{Y1}$ is given by $({}_s\alpha_{Y1})_{II}$ and the rigidity is secured also by Eq.(6.23). Assuming that ${}_fk/{}_sk$ is negligibly small and substituting ${}_sQ_Y = {}_fQ_Y/f$ into Eq.(6.2), the residual plastic deformation in the first story is obtained as

$$\delta_{r1} < \frac{0.2\,\delta_{m1}}{f} \tag{6.24}$$

## 6.2 Lessons Learnt from Hyogoken-Nanbu Earthquake

### 6.2.1 Typical Type of Damage

A common phenomenon found in both the Northridge earthquake (Jan. 17. 1994) and the Hyogoken-nanbu earthquake (Jan. 17. 1995) was unexpected fractural type of failure of steel moment frames [5), 6)]. Steel structural members are composed of plate elements. It has been believed that the maximum strength of the plate elements is generally limited by the local buckling in the plastic range with rare exception in which the maximum strength is determined by the tensile strength of the material. And also it has been believed that the deformation capacity of the plate element limited by breaking under tension is greater than that limited by local buckling under compression.

Typical examples of fracture in the Northridge earthquake are found around the field-weld joint between heavy H-shape columns and deep H-shape beam (Fig.6.4). The flange of beam is welded to the flange of column together with the use of the bolted connection in the web of beam. In such a connection, the bending moment at the web of beam is hardly transmitted to the column, resulting in the stress concentration in flanges at the end of beam. Defects in materials of the heavy column must be an incentive for the propagation of brittle cracks on the side of the column.

Typical examples of fracture in the Hyogoken-nanbu earthquake are found around the weld connection between rectangular-hollow section columns and H-shape beams. While the stress transmission between the beam-flange and the column is made completely through the diaphragm plate, the bending moment in the web of the beam can't be transmitted completely to the column, since the stress transmission is made through the out-of-plane bending of the flange plate of the column. Therefore the stress concentration can occur in the flange of beam. The diaphragm plate is usually

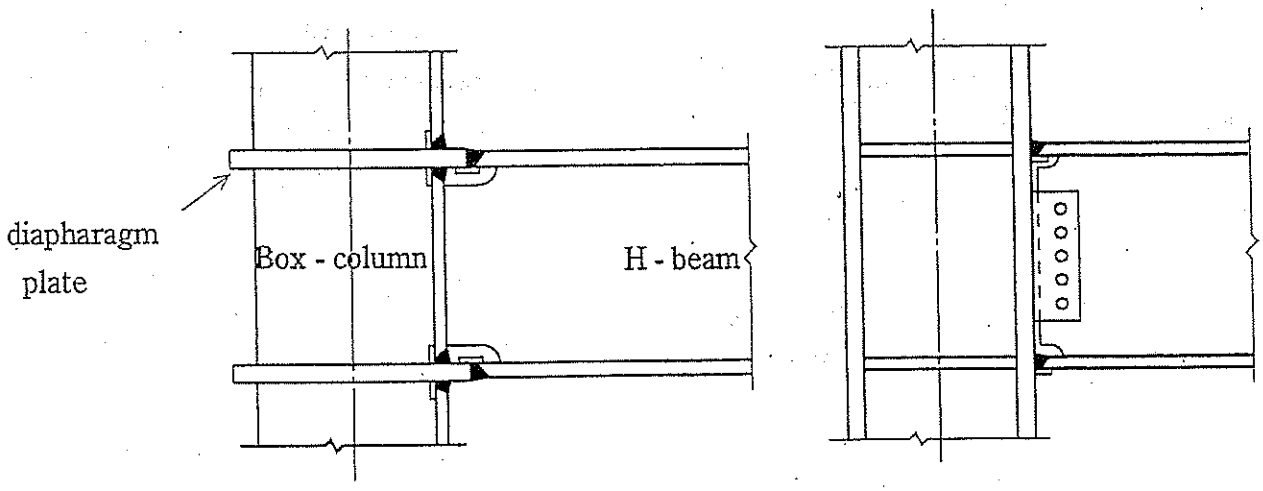


(a) Hyogoken-nanbu Earthquake (b) Northridge

Fig.6.4 Beam-to-Column Connection

thicker and wider than the flange of beam. Then, the fracture develops on the side of beam. As a yield-mechanism, the weak-beam type is preferred both in Japan and USA. This situation characterizes the fracture at the end of beams. In order to secure the deformation capacity of beams, compact beam section with small width to thickness ratios were selected and the stress concentration on flanges at the end of beam hindered the extension of the inelastic region along the beam-axis. These must have brought avoidance of local buckling and revelation of fractural mode of failure in beams. Moreover, an extremely high intensity of the ground motion must be also responsible for such a wide range of damage. In this paper, referring to the current seismic design method in Japan, the following points relevant to the Hyogoken-nanbu earthquake are made clear.

Under what condition could occur the fractural mode of failure of the steel moment frames?

What measure will be effective to prevent the fractural mode of failure?

### 6.2.2 Earthquake Resistant Design Method in Japan

The earthquake resistant design method shown in the Japanese building code which revised in 1981 is summarized as follows.

a) The buildings should be proportioned on the basis of allowable stress design method under the seismic input which corresponds to the intensity level of $C_0 = 0.2$.

b) The building should be equipped with the energy absorption capacity for the seismic input which corresponds to $C_0 = 1.0$.

$C_0$ is a coefficient which indicates the level of seismic input, and the simplified design spectra for $C_0 = 1.0$ are shown in Fig.6.5, specifying ground conditions by I, II and III.

Observing the giving and receiving of the energy input, the basic relationship between the strength for a structure and the seismic input is obtained as shown in Eq.(5.11).

Eq.(5.11) can be rewritten as

$$V_D = \frac{gT\alpha_1}{2\pi}\sqrt{\frac{1+2\eta_1\gamma_1}{\kappa_1}} \tag{6.25}$$

where $V_D = \dfrac{V_E}{1+3h+1.2\sqrt{h}}$

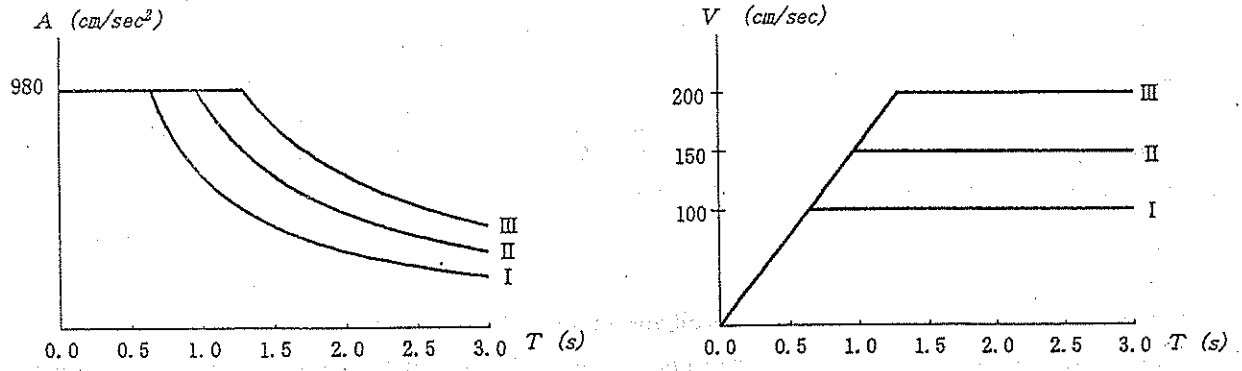


(a) Acceleration Response Spectra (b) Velocity Response Spectra

Fig.6.5 Design Spectra for $C_0 = 1.0$

By applying Eq.(6.25) to existing buildings, we can evaluate the level of seismic input to which the existing building could resist.

### 6.2.3 Condition for Eliminating Brittle Fracture

In 1930s, brittle fracture became most prevailing mode of failure in welded steel ships. The extensive investigation arrived at a conclusion that Charpy impact test can provide a reliable basis to establish a criterion in order to eliminate brittle fracture [7].

Under a certain temperature, the fracture surface of V-notch specimen of Charpy impact test changes into perfectly crystallized one and indicates no trace of ductility. This temperature is defined to be the nilductility temperature, NDT.

As for the criteria to eliminate brittle or unstable fracture, the following conditions have been established for mild steels.

- Under the temperature higher than NDT+15°C, the unstable fracture does not occur under the stress level less than $\sigma_Y/2$, where $\sigma_Y$ is the yield strength of materials.
- Under the temperature higher than NDT+30°C, the unstable fracture does not occur under the stress level less than $\sigma_Y$.
- Under the temperature higher than NDT+60°C, the unstable fracture does not occur under the stress level less than $\sigma_B$, where $\sigma_B$ is the tensile strength of materials.
- NDT+60°C is the temperature limit to eliminate brittle fracture in the plastic range and is defined to be the fracture-transition plastic, FTP.
- NDT+30°C is the temperature limit to eliminate the brittle fracture in the elastic range and is defined to be the fracture-transition elastic, FTE.

In order to develop a sufficient inelastic deformation, the condition for used temperature greater than FTP must be satisfied. Aforementioned criteria for FTP was established for ships. The problem is; what is the criteria for FTP in the seismic design of buildings? In order to grapple with the problem, a full scale shaking table tests become inevitably necessary, since the real situation of stress concentration, strain rate and heat generation accompanied with plastic deformation can be adequately simulated only in the full scale shaking table tests.

The results of full scale shaking tests are summarized as follows [8].

$$\left.\begin{aligned} \text{FTP} &= \text{NDT}+40^\circ\text{C} \\ \text{FTE} &= \text{NDT}+30^\circ\text{C} \end{aligned}\right\} \qquad (6.26)$$

The reason for the reduction of the temperature of FTP in the shaking table tests by 20°C is ascribed to the rise of temperature around the plastified zone due to the rapid development of plastic strains.

### 6.2.4 Ultimate Seismic Resistance of Weak Beam Type Moment Frames

The inelastic deformation capacity for frames which collapse in the fractural mode of failure in beams is estimated under the condition that beams are used under the temperature higher than FTP. The relationship between the applied moment, $M$, and the rotation at the end of beam subjected to the asymmetric moment distribution, $\theta$ becomes such as shown in Fig.6.6. When the maximum strength is limited by local buckling or lateral buckling, the beam can continue to absorb energy in the range of strength deterioration. On the other hand, when the fracture takes place, the energy absorption capacity is limited at the maximum strength point. When buckling does not takes place, the full-plastic moment $M_p$, and the fractural moment, $M_B$, are expressed by

$$\left.\begin{aligned} M_p &= \sigma_Y Z_p \\ M_B &= \sigma_B Z_p \end{aligned}\right\} \qquad (6.27)$$

where $Z_p$ : plastic section modulus

The flexural rigidity in the strain-hardening range of the $M-\theta$ relationship, $D_{st}$ is approximately related to the rigidity in the elastic range, $D$ as follows.

$$D_{st} = 0.03D \qquad (6.28)$$

Approximating the $M-\theta$ relationship with the solid line in Fig.6.6, the cumulative inelastic deformation ratio under monotonic loading, $\bar{\eta}_B$, is expressed by

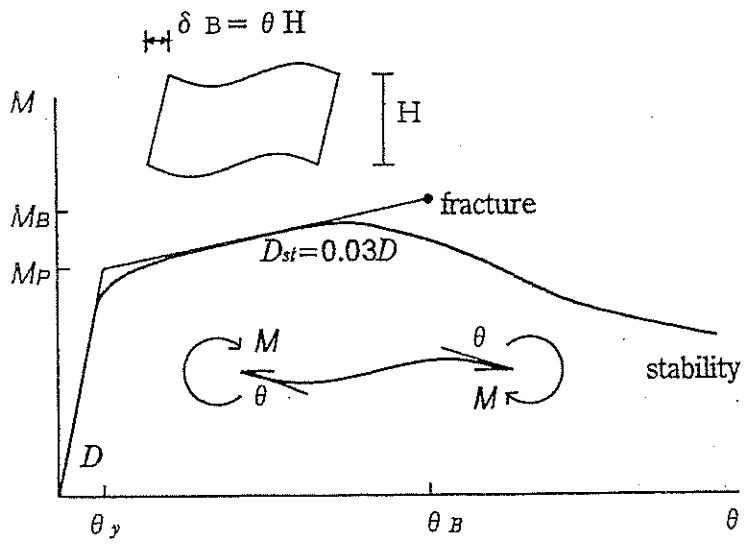


Fig.6.6 $M-\theta$ Relationship of Beam

$$\bar{\eta}_B = \frac{(M_B/M_p)^2-1}{2D_{st}/D} = \frac{(\sigma_B/\sigma_Y)^2-1}{0.06} \tag{6.29}$$

$\bar{\eta}_B$ can be related to $\eta_1$ in Eq.(6.25) as follows

$$\eta_1 = \frac{2\delta_{BY}}{\delta_{Y1}} \cdot a_B \cdot a_p \cdot \bar{\eta}_B \tag{6.30}$$

where $a_B$ : amplification factor due to Bauschinger effect

$a_p$ : amplification factor due to the plastification of structural components other than beams

$\delta_{BY}$ : yield deformation of the first story calculated on the assumption that members other than beams are rigid (see Fig.6.6 in which $H$ is the height of story)

The factor of 2 in Eq.(6.30) corresponds to the assumption that the inelastic deformation takes place with equal amount both in positive and negative directions. Assuming $\delta_{BY}/\delta_{Y1} = 1/3$, $a_B = 2.0$ and $a_p = 1.5$, Eq.(6.30) is reduced to

$$\eta_1 = 2\bar{\eta}_B \tag{6.31}$$

In beam-to-column connections as is shown in Fig.6.4, the transmission of bending moment through the web plate of beam is incomplete, and an effective section modulus, $Z_{pe} = rZ_p$ must be introduced to estimate the maximum strength, $M_B$, as follows.

$$Z_{pe} = rZ_p \tag{6.32}$$

$$r = \frac{A_f + r_w A_w/4}{A_f + A_w/4} \tag{6.33}$$

where $r$ : reduction factor of the section

$r_w$ : reduction factor of the web

$A_f$ : area of the flange (one side)

$A_w$ : area of the web

In such a case, $\bar{\eta}_B$ becomes

$$\bar{\eta}_B = \frac{(r\sigma_B/\sigma_Y)^2-1}{0.06} \tag{6.34}$$

Beams are generally connected to concrete slabs with stud bolts. In such a composite beams, since the plastification of upper flange of beams is not likely to occur under the bending moment which produces a compressive stress in the concrete slab, the energy absorption capacity of beams can be reduced to three fourths of the original. Considering such a situation, the ultimate seismic resistibility of the moment frames is evaluated on the basis of Eq.(6.25). As a practical example, the following conditions are taken.

structures : $\delta_Y = \frac{H}{150}$, $H = 400cm$ ; $n = 6$ (weak beam type)

material : $\sigma_Y = 1.2\sigma_{Y0}$, $\sigma_B = 1.1\sigma_B$

$$\left(\begin{array}{l}\sigma_Y = 3.3t/cm^2,\ \sigma_{B0} = 5.0t/cm^2 \\ \text{specificated values for SM490 steels}\end{array}\right)$$

others : $h = 0.02$

From Fig.6.5, the shear force coefficient used for the allowable stress design, $\alpha_e$, is read as follows.

$$\left.\begin{array}{l} \text{For } T \leq 1.28\text{sec},\ \alpha_e = 0.2 \\ \text{For } T > 1.28\text{sec},\ \alpha_e = \dfrac{0.256}{T} \end{array}\right\} \tag{6.35}$$

Since the skeletons are designed on the basis of the elastic analysis, the strength which corresponds to $\alpha_e$ is the elastic limit strength, $Q_{e1}$. The yield strength, $Q_{Y1}$, and $Q_{e1}$ can be roughly related to be

$$Q_{Y1} \geq 1.5 Q_{e1} \tag{6.36}$$

Therefore, considering also the increase of yield point stress by 20 percents, $\alpha_1$ can be assumed to be

$$\alpha_1 = 1.5 \times 1.2 \alpha_e = 1.8 \alpha_e \tag{6.37}$$

The fundamental natural period $T$ is written as

$$T = 2\pi \sqrt{\frac{M}{k_{eq}}} = 2\pi \sqrt{\frac{M\kappa_1}{k_1}} \tag{6.38}$$

Knowing $k_1 = Q_{y1} / \delta_{y1} = \alpha_1 Mg / \delta_{Y1}$, $T$ is reduced to

$$T = 2\pi \sqrt{\frac{\kappa_1 \delta_{Y1}}{\alpha_1 g}} \tag{6.39}$$

Applying Eqs.(6.29) and (6.31) for the given condition,

$$\eta_1 = 31.0 \tag{6.40}$$

For reference's sake, two other values of $\eta_1$ are taken, i.e. $\eta_1 = 20.0$ and $\eta_1 = 10.0$. Values of $r$ and $r_w$ which corresponds to the selected values of $\eta_1$ are obtained as follows by applying Eqs.(6.32) and (6.33) and practical values of $A_f / A_w$ ranging from 1.0 to 2.0.

For $\eta_1 = 20.0$, $r = 0.91$, $r_w = 0.55 \sim 0.73$

For $\eta_1 = 10.0$, $r = 0.82$, $r_w = 0 \sim 0.46$

Considering the influence of composite-beam action, $\eta_1$ factored by 0.75 is also applied. $V_D$-values obtained by Eq.(6.25) are shown in Fig.6.7. $V_D$-spectra along the fault line of the Hyogoken-nanbu earthquake are indicated by three bi-linear curves according to the classification of ground and the $V_D$-spectrum for the record at Kobe Meteorological Observatory by Japan Meteorological Agency (JMA) is also shown. The bi-linear relationship shown by broken line is the $V_D$-spectrum on the soft ground prescribed in Japanese Building Code.

Comparing the intensity of the seismic input and the capacity of frames, the following facts can be seen form Fig.6.7.

1) The maximum intensity of the seismic input in the Hyogoken-nanbu Earthquake was one point five to two times as large as the intensity prescribed in the current Japanese Building Code.
2) The deficiency of the moment-transmission through the web plate at the beam-to-column connection governs the deformation capacity of the beam.

3) The allowable stress design under the seismic input of $C_0 = 0.2$ is very effective to secure a minimum required level of strength of frames.

4) Under the condition of $r_w > 0.5$, $\eta_1$ reaches the level of 20.0. Therefore, it can be said that the fractural mode of failure could be avoided by applying the current design method as far as the condition of $r_w > 0.5$ is kept.

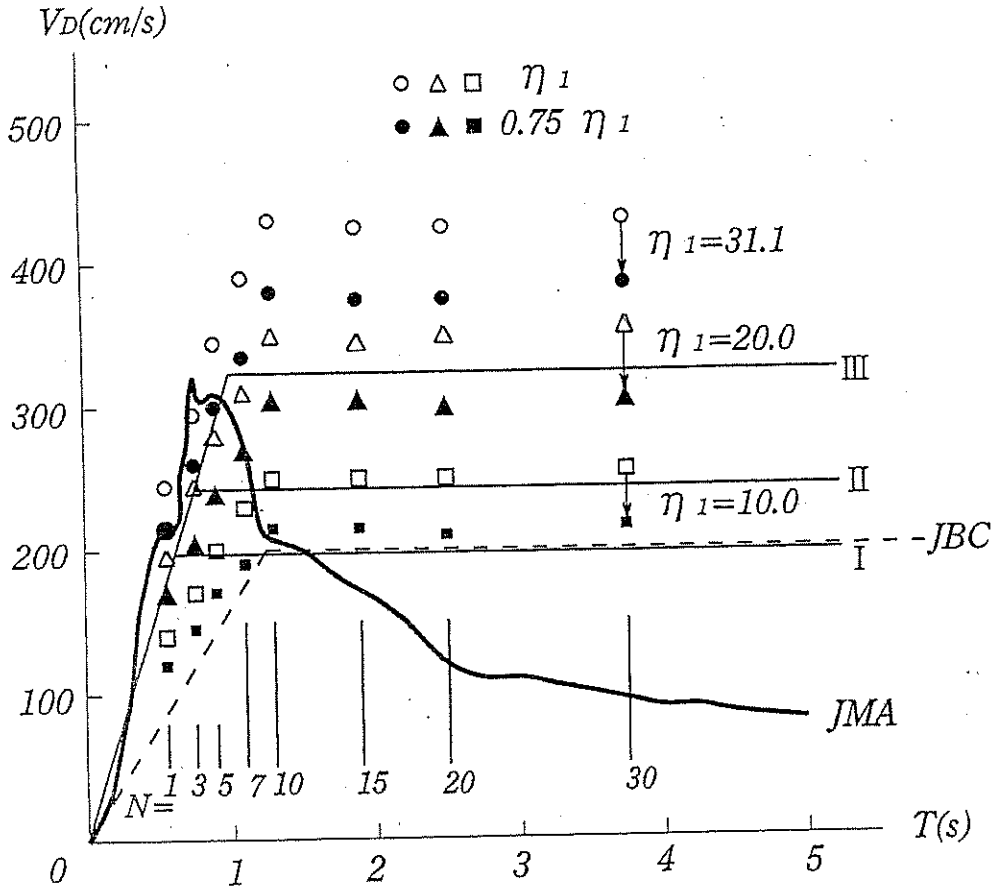


Fig.6.7 $V_D - T$ Relationship

## References


1) Akiyama, H.: Earthquake-Resistant Limit-State Design for Buildings, University of Tokyo Press, 1985

2) Housner, G. W.: Limit Design of Structures to Resist Earthquakes, Proc. of 1st WCEE, 1956

3) housner, G. W.: Behavior of Structures during Earthquakes, ASCE, EM4, Oct. 1959.

4) Akiyama, H.: Earthquake-Resistant Design Method for Buildings Based on Energy Balance, Gihodoshuppan, 1999. (In Japanese)

5) Akiyama, H. and Yamada, S.: Seismic Input and Damage of Steel Moment Frames, Stessa '97, Kyoto, Japan, 3-8 August, 1997

6 ) Engelhardt, M. D. and Sabol, T. A.: Testing of Welded Steel Moment Connections, in Response to the Northridge Earthquake, Progress Report to the AISC advisory Subcommittee on Spècial Moment Resisting Frame Research.
7 ) Tetelman, A. S. and McEvily, A. J.: Fracture of Structural Materials, John Wiley & Sonns, Inc. 1967
8 ) Akiyama, H., Yamada, S, Minowa, C., Teramoto, T., Otake, F. and Yabe, Y.: Experimental Method of the Full Scale Shaking Table Test Using the Inertial Loading Equipment, J. Struct. Constr. Eng., AIJ, No.515. (In Japanese)